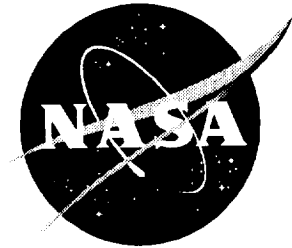


NASA/CR-1999-209120/VOL3



Acoustic Treatment Design Scaling Method

Volume 3: Test Plans, Hardware, Results, and Evaluation

J. Yu, H. W. Kwan, and D. K. Echternach
Rohr, Inc., Chula Vista, California

R. E. Kraft and A. A. Syed
General Electric Aircraft Engines, Cincinnati, Ohio

National Aeronautics and
Space Administration

Langley Research Center
Hampton, Virginia 23681-2199

Prepared for Langley Research Center
under Contract NAS3-26617, Task 25

April 1999

Available from:

NASA Center for AeroSpace Information (CASI)
7121 Standard Drive
Hanover, MD 21076-1320
(301) 621-0390

National Technical Information Service (NTIS)
5285 Port Royal Road
Springfield, VA 22161-2171
(703) 605-6000

Abstract

The ability to design, build, and test miniaturized acoustic treatment panels on scale model fan rigs representative of the full scale engine provides not only a cost-saving but an opportunity to optimize the treatment by allowing tests of different designs. To be able to use scale model treatment as a full scale design tool, it is necessary that the designer be able to reliably translate the scale model design and performance to an equivalent full scale design.

The primary objective of the study presented in this volume of the final report was to conduct laboratory tests to evaluate liner acoustic properties and validate advanced treatment impedance models. These laboratory tests include DC flow resistance measurements, normal incidence impedance measurements, DC flow and impedance measurements in the presence of grazing flow, and in-duct liner attenuation as well as modal measurements. Test panels were fabricated at three different scale factors (i.e., full-scale, half-scale, and one-fifth scale) to support laboratory acoustic testing. The panel configurations include single degree of freedom (SDOF) perforated sandwich panels, SDOF linear (wire mesh) liners, and double degree of freedom (DDOF) linear acoustic panels.

Six sets of acoustic test samples with fifteen liner configurations, and three scale factors were fabricated and tested. The DC flow resistance measurements and normal incidence impedance tests have provided useful data to support scale treatment impedance analytical model development and validation. The analyses demonstrate that the theoretical impedance models discussed can be upgraded and modified to fit both full-scale and sub-scale liners requirements.



Table of Contents

1. Introduction	1
2. Fabrication of Test Specimens	2
2.1 Test Matrix	2
2.2 Fabrication Approach	2
2.2.1 Material Selection (Framed and Instrumented Panels)	2
2.2.2 Bonding Methods	4
2.3 Quality Assurance.....	4
3. Acoustic Tests.....	6
3.1 Test Facilities	6
3.2 DC Flow Resistance Measurement.....	6
3.2.1 Measuring System and Calibration	6
3.2.2 DC Flow Resistance Testing	7
3.3 Normal Incidence Acoustic Impedance Measurement	8
3.3.1 Measuring Systems and Calibration.....	8
3.3.2 Non-destructive Acoustic Impedance Test	8
3.3.3 Destructive (In-tube) Normal Incidence Acoustic Impedance Test.....	11
4. Data Analysis and Evaluation	14
4.1 Basic Impedance Mathematical Model Description	14
4.2 Effective POA and Hole Diameter Estimate.....	16
4.2.1 Methods for Estimating Effective POA and Hole Diameter	16
4.2.2 Perforated Liner Effective POA and Hole Diameter	19
4.3 Normal Incidence Impedance Measurement Data.....	21
4.3.1 Data Analysis and Evaluation Approach.....	21
4.3.2 SDOF Perforate Plate Liner Impedance Data Analysis.....	22
4.3.3 SDOF and DDOF Linear Liner Impedance Data Analysis.....	33
5. Conclusions and Recommendations	45
6. Appendix A - Acoustic Test Specimen Matrices	46
7. Appendix B - Inspection Plan	58
8. Appendix C - High Temperature DC Flow Resistance Tests	59
8.1 Steady (DC) Flow Resistance Testing.....	59
8.2 High Temperature DC Flow Resistance Tests.....	60
8.3 Calibration of the Apparatus	61
8.3.1 Critical flow nozzles.....	61
8.3.2 Pressure Sensors.....	61
8.3.3 Temperature Gages.....	62

8.4 Test Procedure.....	62
8.5 Test Results.....	64
9. Appendix D - Technical Issues for Fabrication of Treatment Samples.....	72
9.1 Micro-perforated Specimens.....	72
9.2 Flow Duct Frames.....	72
9.3 Plexiglass Bonding.....	72
9.4 Instrumentation.....	73

1. Introduction

Various laboratory tests were conducted to evaluate liner acoustic properties and validate advanced treatment impedance models. These laboratory tests included DC flow resistance measurements, normal incidence impedance measurements, DC flow and impedance measurements in the presence of grazing flow, and in-duct liner attenuation including modal measurements. The first two tests were performed at Rohr Inc., and the remaining tests were conducted by GEAE. Based on each test requirement, specific test panels were fabricated at three different scale factors (i.e., full-scale, half-scale, and one-fifth scale) to support laboratory acoustic testing. The panel configurations include single degree of freedom (SDOF) perforated sandwich panels, SDOF linear (wire mesh) liners, and double degree of freedom (DDOF) linear acoustic panels. The bulk absorber liner that was considered in the original plan was eliminated due to cost restrictions.

The fabrication of test specimens for all test programs is briefly described in Section 2. Testing other than the testing in the grazing flow duct is the subject of this volume. Acoustic laboratory testing for normal incidence impedance tube and DC flow resistance measurements is explained in Section 3. Test data reduction and analyses are presented in Section 4 while conclusions and recommendations are discussed in Section 5. The grazing flow duct tests, including modal measurements and grazing flow DC flow resistance measurements and their analysis is the subject of Final Report Volume 5. Acoustic test specimen matrices and Quality Assurance Inspection Plan are provided in Appendix A and Appendix B. The results of the high temperature DC flow resistance testing are included in Appendix C. Additional discussion of fabrication for the treatment test panels is included in Appendix D.

Validation of the advanced treatment impedance models without grazing flow present was accomplished through the use of DC flow and normal incidence acoustic impedance measurements. The study indicates that the impedance model described in Volume 2 of the final report, with additional refinements, can accurately predict acoustic impedance for both full-scale and sub-scale acoustic treatments. These refinements include using DC flow resistance to estimate effective percent open area (POA) and hole diameter values, using an empirical data base to determine the discharge coefficient, and introducing a non-linear mass reactance factor to correct for end effects.

Validation of the advanced treatment impedance models with grazing flow present was not completed due to difficulties of measuring in-duct liner impedance and modal distributions at high frequencies. In the future, more advanced techniques to measure acoustic impedance in the high frequency range should be developed with and without grazing flow.

2. Fabrication of Test Specimens

2.1 Test Matrix

A primary goal of this program is to establish the impedance relationship between full-scale and sub-scale panels that have near exact geometrical scaling factors. The test matrix that addresses this goal includes seven groups of liner specimens with target liner configurations for each group shown in Table 2-1. Due to cost restrictions, the bulk absorber liner listed in Group 7 was eliminated. A detailed matrix that shows material selection, sample dimensions (including frames), instrumentation requirements, and function of the test panels is provided in Appendix A. Further discussion of test panel fabrication is included in Appendix D.

Table 2-1 Target Liner Configurations of Acoustic Test Specimens

Group ID	Liner Type	Liner R(105)	POA	Hole Diameter	Plate Thickness	Core Depth	Scale Factor
1-1	SDOF Perf.	--	10.0	0.039"	0.025"	1.00"	1
1-2	SDOF Perf	--	10.0	0.020"	0.012"	0.50"	1/2
1-3	SDOF Perf	--	10.0	0.008"	0.005"	0.20"	1/5
2-1	SDOF Perf.	--	12.0	0.051"	0.032"	1.00"	1
2-2	SDOF Perf	--	12.0	0.025"	0.016"	0.50"	1/2
2-3	SDOF Perf	--	12.0	0.016"	0.006"	0.20"	1/5
3-1	SDOF Perf.	--	8.0	0.039"	0.025"	1.00"	1
3-2	SDOF Perf	--	8.0	0.020"	0.012"	0.50"	1/2
3-3	SDOF Perf	--	8.0	0.008"	0.005"	0.20"	1/5
4-1	SDOF Linear	90 rayl	34.0	0.05"	0.025"	1.00"	1
4-2	SDOF Linear	90 rayl	--	--	--	0.20"	1/5
5-1	SDOF Linear	60 rayl	34.0	0.05"	0.025"	1.00"	1
5-2	SDOF Linear	60 rayl	--	--	--	0.20"	1/5
6-1	DDOF - Face	40 rayl	34.0	0.05"	0.025"	0.90"	1
	- Septum	100 rayls	34.0	0.05"	0.025"	1.50"	1
6-2	DDOF - Face	40 rayl	--	--	--	0.18"	1/5
	- Septum	90 rayls	--	--	--	0.30"	1/5
7-1	Bulk Liner	100 rayl/cm	34.0	0.05"	0.02"	1.00"	1
7-2	Bulk Liner	200 rayl/cm	34.0	0.05"	0.02"	0.50"	1/2
7-3	Bulk Liner	500 rayl/cm	34.0	0.05"	0.02"	0.21"	1/5

2.2 Fabrication Approach

2.2.1 Material Selection (Framed and Instrumented Panels)

Treatment panel samples were mounted in frames such that they could be installed in the GEAE flow duct facility for grazing flow duct testing. Figure 2-1 is a drawing of the treatment panel sample mounted in the duct test frame. Special consideration was given to material selection used on framed and instrumented panels. Hardwood select maple was used for frame construction due to advantages in weight, dimensional stability, and machineability. Assembly of the wood frames was achieved through the use of wood dowels and carpenter's glue.

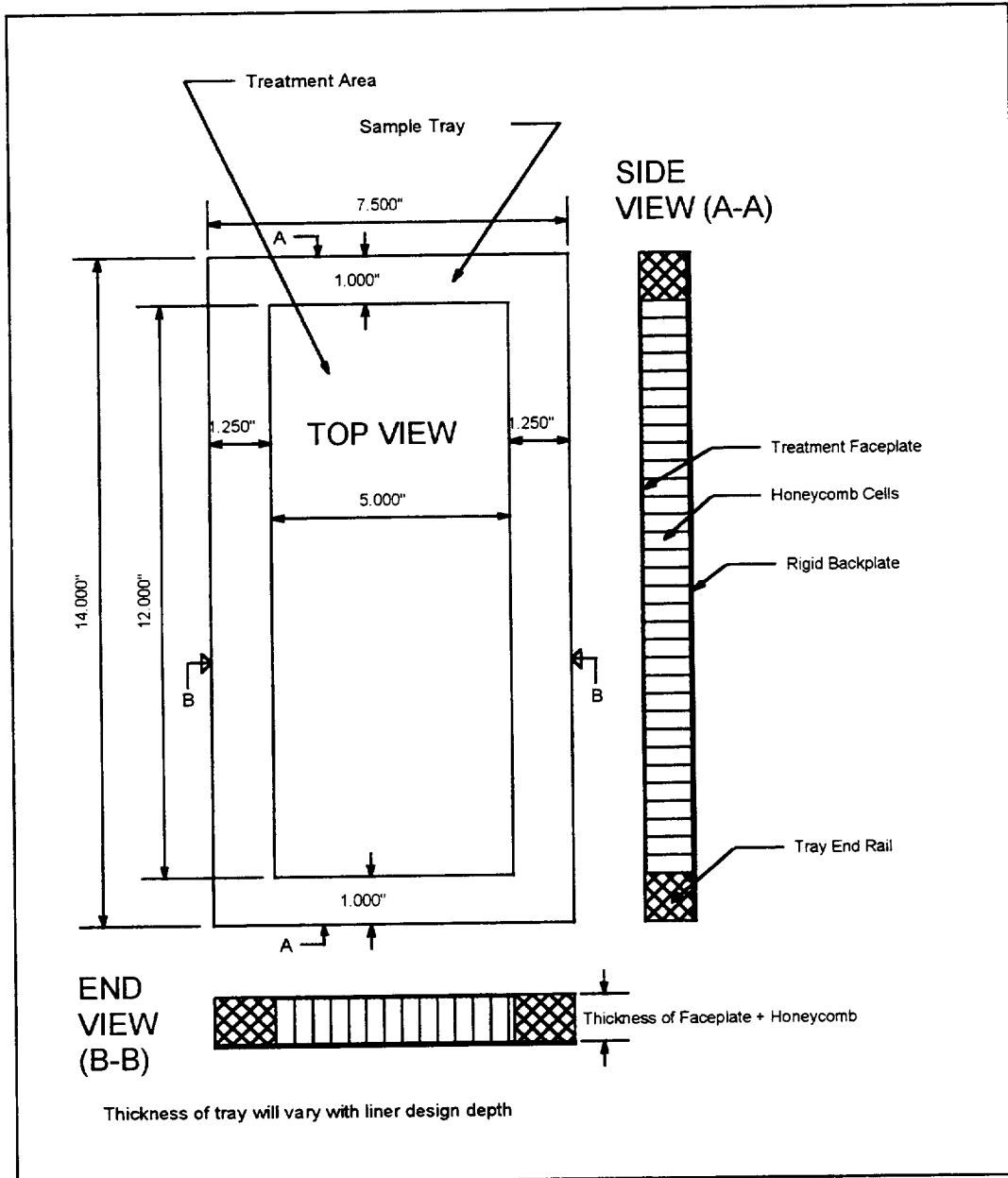


Figure 2-1 Treatment Panel Sample Mounted in Duct Test Tray

Instrumented panels required special consideration for Plexiglas-to-core bonding. Several materials were evaluated for their ability to adhere to the Plexiglas and to provide suitable visual qualities required for the placement of Kulite tubes. A room temperature cure product was also necessary. EnviroTex Lite polymer coating conforming to ASTM D 4236 was selected to best fit the above criteria.

Instrumented panel partitions also required special consideration for fabrication and installation. It was decided to use .062" aluminum sheet which was sheared to size then brazed on a weld jig for dimensional control. Each partition was processed then primed prior to

installation. Core cutting dies (inner and outer) were fabricated and used to cut the honeycomb core allowing sufficient clearance for tray placement and bonding. A schematic of an instrumented panel is shown in Figure 2-2.

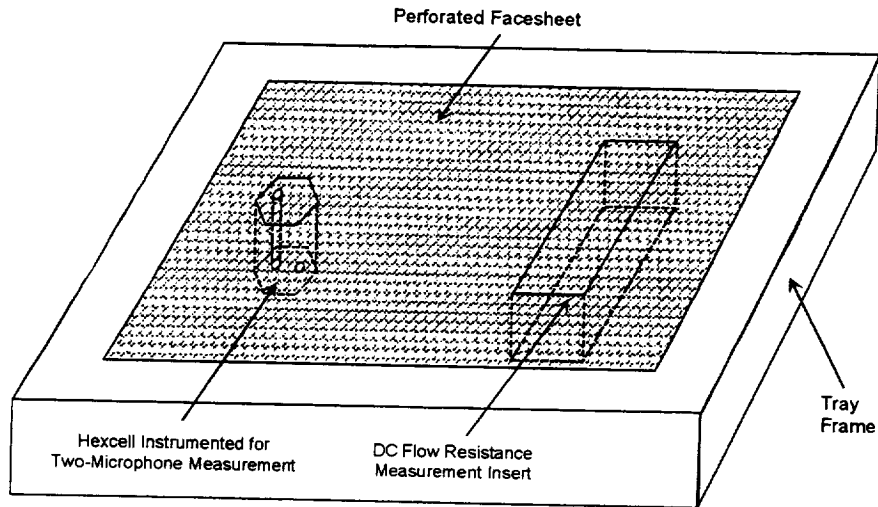


Figure 2-2 Schematic of Instrumented Treatment Test Panel Mounted in Tray

2.2.2 Bonding Methods

Rohr standard bonding practices were employed implementing minor variations in technique to accommodate various core cell sizes and perforate percent open area (POA) for fabrication of the acoustic honeycomb test panels. RMS 058 supported and unsupported 350° epoxy adhesives were utilized for core-to-skin bonding. Adhesive reticulation techniques varied based on POA and hole diameter of the perforated acoustic skin. Skin processing prior to bonding included sulfuric boric anodize (for perforated skins) and phosphoric acid anodize (for solid backskins) followed by application of RMS 058 Type 5 primer.

Process procedures were controlled utilizing a Fabrication Planning Request Form which was specifically developed for this program. This form was implemented due to the quantity of panels to be manufactured (42) and the similarity of materials and processing methods employed for fabrication. The two page form consisted of a sketch of the panel configuration, list of materials required, and a check-off list of processes to be used for fabrication of each individual panel. Use of this format proved to be successful in reducing redundant instructions into a condensed "user friendly" planning document.

2.3 Quality Assurance

Quality Assurance provisions for the Acoustic Scaling Model Program were established through joint agreement with GEAE and Rohr (See Appendix B). Program critical elements such as material traceability, dimensional tolerances, acoustic testing, NDE, and final inspection reports were controlled and documented on the "Acoustic Panel Request Form".

Acoustic testing was accomplished at each step of the bond process to ensure acoustic conformity of the final bond panel. To ensure dimensional conformity of each flow duct tray, each was "custom fit" to accommodate the various acoustic panel thicknesses, then assembled, and finally machined to the required dimensions. Final buy-off of each panel was based on a review of the final package including planning, material traceability, compliance to process, acoustic test results, and dimensional conformity.

3. Acoustic Tests

3.1 Test Facilities

Rohr has a variety of acoustical test facilities to support theoretical analyses, advanced liner development, and acoustic liner design evaluations. These include:

- 10 cm diameter automated laboratory Raylometer at Riverside;
- 10 cm diameter low-frequency sound impedance measuring system (.2k-1.6k Hz);
- 3 cm diameter 8 Hz bandwidth sound impedance measuring system (.8k-6k Hz);
- 1.5 cm diameter high-frequency sound impedance measuring system (3k-13k Hz).

A two-microphone technique and random noise signal are used in all Rohr impedance measuring systems.

3.2 DC Flow Resistance Measurement

3.2.1 Measuring System and Calibration

The steady state airflow resistance of the test panels at each step of the assembly process was measured using Rohr Riverside's Engineering Laboratory Raylometer. This apparatus, which has a 10 cm diameter test port, is shown in Figure 3-1. For all measurements, flow resistance was measured at airflow velocities of 30, 60, 105, 150 and 200 cm/sec and a first order least squares curve fit of the resistance as a function of velocity was determined at each point. All data are corrected to reference ambient conditions of 70°F and 29.92 inch Hg. These measurements are used to demonstrate compliance with the manufacturing tolerances for each configuration.

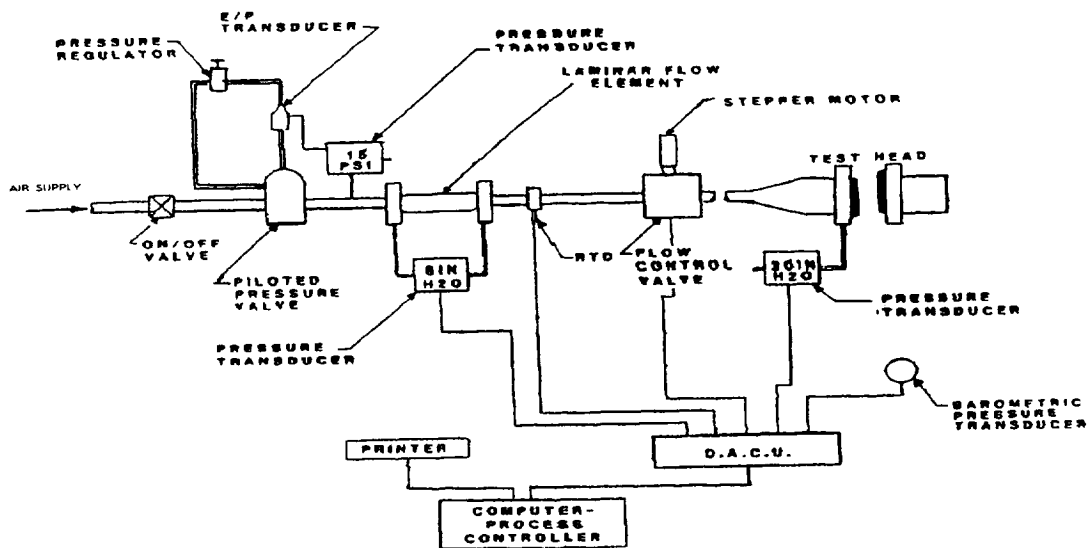


Figure 3-1 DC flow resistance measuring system

3.2.2 DC Flow Resistance Testing

The number of test locations for each liner is defined by the size of the liner. For SDOF perforate liners, the DC flow resistance of a perforate bonded to core was measured. For SDOF linear liners, the DC flow resistance of wire mesh bonded to core or wire mesh bonded to the perforate plate and core was measured. For DDOF liners, the DC flow resistance of the face sheet and septum were measured separately. Table 3-1 lists the measured DC flow resistance at a velocity of 105 cm/sec and the respective non-linear factor (NLF), i.e., $R(200)/R(20)$. The measured DC flow resistance of SDOF perforate liners is used to calculate a percentage open area (POA) of the perforate plate (see Section 4.2). For DDOF liners, the measurements meet the specifications listed in Table 2-1.

Table 3-1 Measured DC Flow Resistance of Acoustic Test Specimens

Group ID	Liner Type	Liner R(105) (Rayls)	NLF	Scale Factor
1.1-1	SDOF Perf.	12.25	7.14	1
1.1-2	SDOF Perf	11.16	6.80	1
1.2-1	SDOF Perf	9.92	7.34	1/2
1.2-3	SDOF Perf	9.44	7.30	1/2
1.3-1	SDOF Perf	12.53	5.68	1/5
1.3-2	SDOF Perf	8.29	5.23	1/5
2-1	SDOF Perf.	5.96	7.74	1
2-3	SDOF Perf	7.52	7.68	1/2
2-5	SDOF Perf	6.96	6.17	1/5
3-1	SDOF Perf.	13.73	6.45	1
3-3	SDOF Perf	15.68	7.82	1/2
3-5	SDOF Perf	11.65	6.34	1/5
4-1	SDOF Linear	84.53	1.40	1
4-2	SDOF Linear	88.20	1.32	1
4-4	SDOF Linear	83.43	1.15	1/5
5-1	SDOF Linear	56.82	1.48	1
5-4	SDOF Linear	48.68	1.21	1/5
6-1	DDOF - Face	46.35	1.51	1
	- Septum	89.32	1.61	1

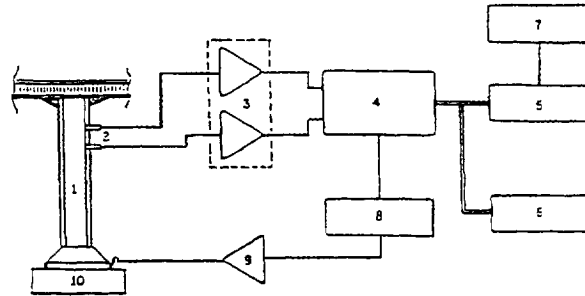
3.3 Normal Incidence Acoustic Impedance Measurement

3.3.1 Measuring Systems and Calibration

Pressure transducer sensitivities, for both the acoustic impedance measuring system and the acoustic insertion loss measuring system, are calibrated in accordance to Rohr Report RHR 89-191, "Calibration System Used in the Engineering Test Laboratories." The amplitude and phase calibration for the two-microphone impedance system transducers are performed in accordance to the method described in the ASTM E1050-90 impedance measurement standard.

3.3.2 Non-destructive Acoustic Impedance Test

A two-microphone impedance measuring system was used to conduct all acoustic impedance measurements. A block diagram of the Rohr acoustic impedance measuring system is shown in Figure 3-2.



1. 3 cm impedance tube.
2. Kulite pressure transducer.
3. Microphone pre-amplifiers.
4. Dual channel signal analyzer.
5. Computer.
6. Graphics plotter.
7. Printer
8. Bandpass filter.
9. Power amplifier.
10. High power compression driver.

Figure 3-2 Schematic of the Rohr acoustic impedance system

A test sample was installed at one end of the impedance tube as a termination (see Figures 3-3 and 3-4). Using a random noise excitation, the normal specific acoustic impedance of the test sample was determined from two pressure measurements along the wall of the impedance tube. The results were used to validate Rohr's analytical impedance prediction code.

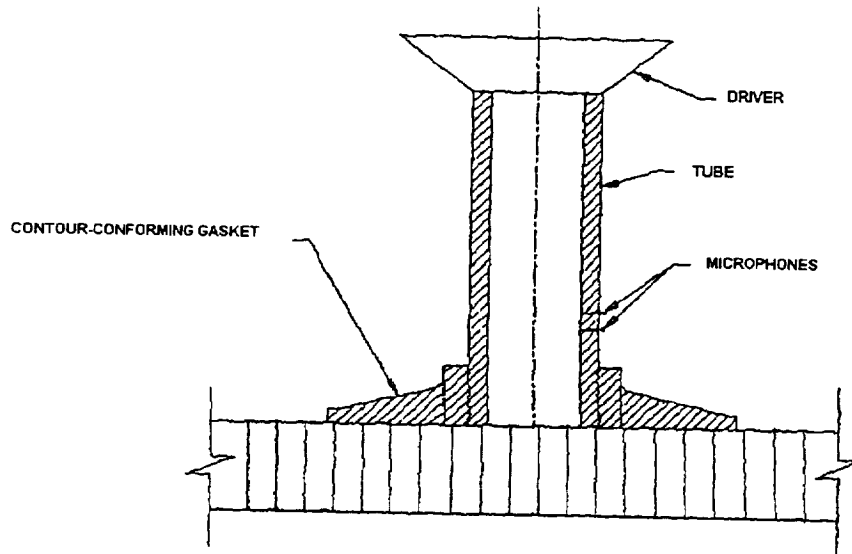


Figure 3-3 Test setup for single degree of freedom liner panel measurement

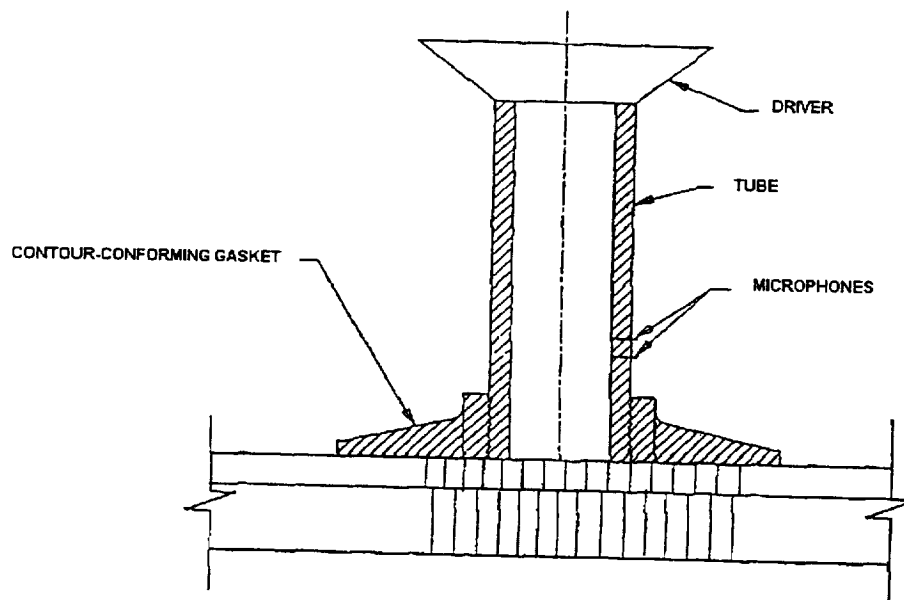


Figure 3-4 Test setup for double degree of freedom liner panel measurement

The frequency for this test ranges from 800 to 6000 Hz. Overall sound pressure levels (OASPL) of up to 160 dB can be achieved at the face of the test sample. The characteristics of this pressure spectrum are documented for use in the corresponding acoustic impedance calculations. For each test sample, three test levels that range from 130 dB to 160 dB were used. The measured and calculated acoustic impedance data is provided in 120 Hz bandwidth narrow band form. The results of non-destructive acoustic impedance tests are presented and discussed in Section 4.

3.3.3 Destructive (In-tube) Normal Incidence Acoustic Impedance Test

Figure 3-5 shows an area mismatch due to the honeycomb cell size for the non-destructive acoustic impedance test. This allows some acoustic energy to dissipate into the structure of double layer liners with unaligned core. In an attempt to avoid this energy leakage, a destructive (in-tube, i.e., free of energy loss) acoustic impedance test was used. Figures 3-6 and 3-7 show the setup of the destructive acoustic impedance test for single degree of freedom (SDOF) liners and double degree of freedom (DDOF) liners. The in-tube samples were cut from the panel. For DDOF liners, a septum was separated from a face sheet, with a spacer height equal to the upper core depth. The bottom core depth can be adjusted by the micrometer's moving piston (see Figure 3-7). The rest of test setup is the same as the non-destructive acoustic impedance test. The test results of the destructive acoustic impedance tests (normal incidence) are presented and discussed in Section 4.

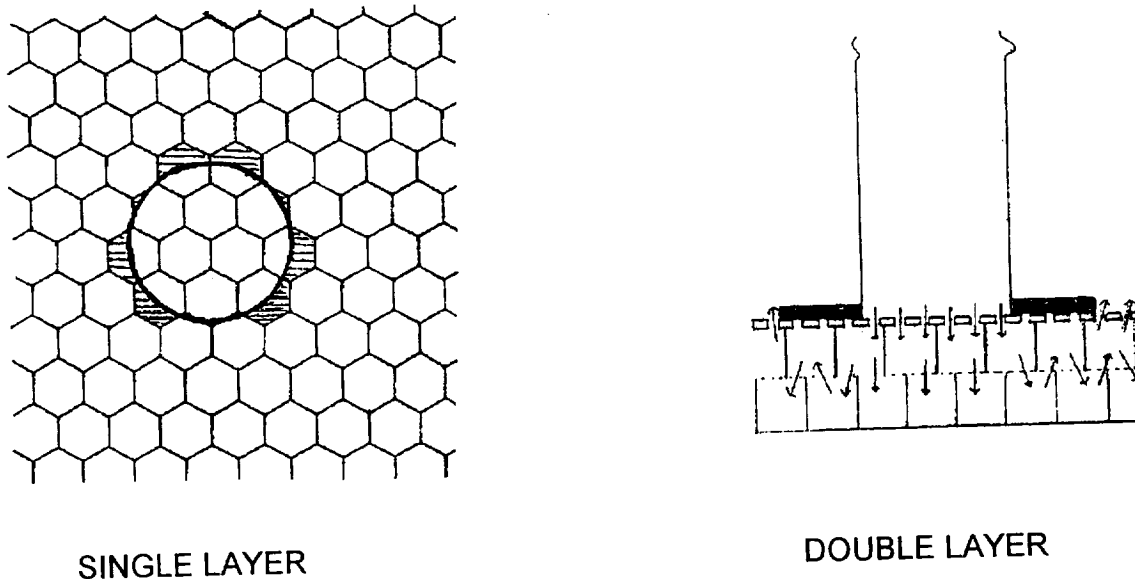


Figure 3-5 Schematic of area mismatch due to honeycomb structure

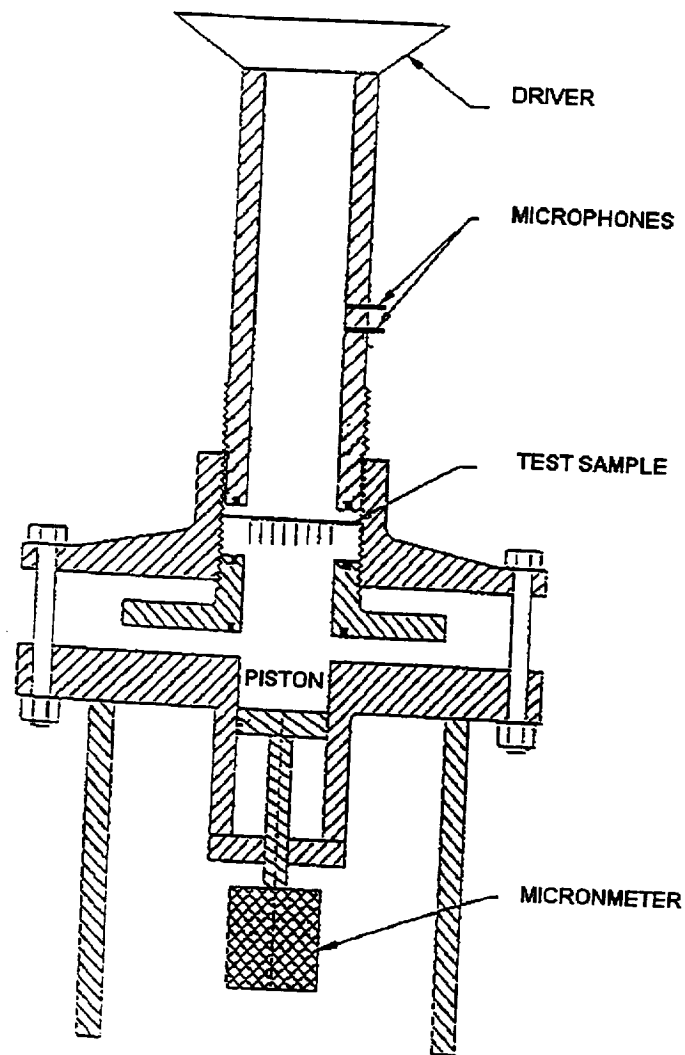


Figure 3-6 Test setup for single degree of freedom liner in-tube measurement

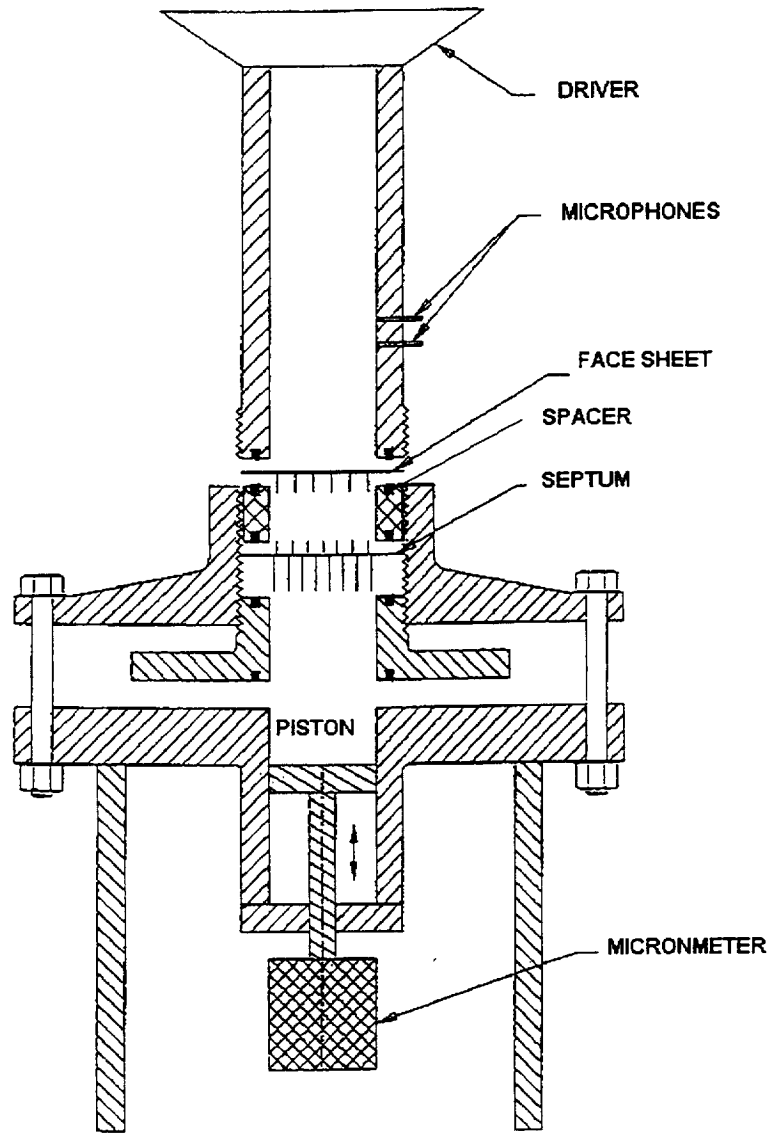


Figure 3-7 Test setup for double degree of freedom liner in-tube measurement

4. Data Analysis and Evaluation

4.1 Basic Impedance Mathematical Model Description

The impedance model used for this effort is based on the theories described in Volume 2 and the empirical data base developed at Rohr and the aerospace industry. We are now switching to the $e^{+i\omega t}$ time convention customarily used by treatment designers. A general impedance model for both the perforate and linear liners can be expressed as follows:

$$\frac{Z_f}{\rho c} = R + iX = R_0 + R_{0f} + S_r V_p + R_{cm}(V_{cm}) + i[X_m + S_m V_p + X_{cm}(V_{cm}) - \cot(kh)] \quad (4-1)$$

where

$Z_f/\rho c$ is a complex number representing normalized impedance at a frequency f .

R is the normalized acoustic resistance

i is $\sqrt{-1}$ (imaginary number)

X is the normalized acoustic reactance

ρ is the air density and c is the sound speed

ρc is defined as characteristic impedance (unit: cgs- Rayl)

R_0 is the non-frequency dependent linear acoustic resistance

R_{0f} is the frequency dependent linear acoustic resistance

S_r is the non-linear resistance slope

V_p is the root-mean-square (rms) particle velocity over the entire frequency range in cm/sec.

From Volume 2, Equation 2-16, $V_p = \sqrt{\sum (V_{pf})^2}$ where $(V_{pf})^2$ is the mean square velocity at frequency f .

V_{cm} is the Mach Number

$R_{cm}(V_{cm})$ is the grazing flow induced acoustic resistance

X_m is the mass reactance

S_m is the non-linear mass reactance slope

$X_{cm}(V_{cm})$ is the mass reactance end correction (including flow effect)

k is the wave number per inch or cm

h is the cavity backing depth in inches or cm

$-\cot(kh)$ is the backing cavity reactance

For perforate plate liners (including both punched and laser drilled sheets), Rohr uses Crandall's model, described in Volume 2, Section 4.1, to calculate the linear and frequency dependent acoustic impedance $Z_0/\rho c$ parameters. These include R_0 (linear resistance), R_{0f}

(frequency dependent resistance), and X_m (mass reactance). The complex equation can be expressed as

$$\frac{Z_{of}}{\rho c} = (R_0 + R_{of}) + iX_m = i\omega \frac{t + \epsilon d}{c\sigma} \frac{1}{F(k_s' r)} \quad (4-2)$$

where

- t is the facesheet thickness
- d is the hole diameter
- σ is the facesheet percent open area (POA or porosity)
- c is the speed of sound
- ω is the circular frequency
- ϵ is the end correction coefficient
- k_s' is the Stokes wave number
- r is the hole radius

Equation (4-2) is slightly different from Equation (4-1) in Volume 2. The first difference is that the end correction shown in Volume 2, Equations 2-23 and 2-24, is added to the component of thickness ($\epsilon d = 0.85d (1 - 0.7\sqrt{\sigma}) / (1 + 305 (V_{cm})^3)$). The FOK function mentioned in Volume 2, Equation (4-13) is not used to estimate the end correction. For each perforate plate, the value of ϵ may be varied slightly due to differences in material selection and hole drilling methods. As a result, an empirical adjustment may be required to obtain a correct constant to estimate the value of ϵ .

An additional difference is the elimination of the discharge coefficient parameter in the Crandall Model. The non-linear resistance slope, S_r , used in these calculations is similar to Melling's expression (Volume 2, Equation (3-1)); however, the factor between the acoustic resistance and DC flow resistance is 1.336541 determined from Rohr's empirical results instead of 1.2 recommended by Melling (Volume 2, Equation (4-20)) or 1.14 suggested by Mariano and by Armstrong, as reported in Zorumski and Tester¹.

The modified Equation for the nonlinear resistance slope is

$$S_r = 1.336541 \left(\frac{\rho}{2C_D^2} \frac{1 - \sigma^2}{\sigma^2} \right) \quad (4-3)$$

which can be compared to

$$S = \left(\frac{\rho}{2C_D^2} \frac{1 - \sigma^2}{\sigma^2} \right) \quad (4-4)$$

¹ Zorumski, William E. and Tester, Brian J., "Prediction of the Acoustic Impedance of Duct Liners", NASA TM X-73951, September, 1976, pp. 14-15.

for the DC flow resistance slope. The discharge coefficient is

$$C_D = 0.80695 \sqrt{\frac{\sigma^{0.1}}{e^{-0.5072\left(\frac{t}{d}\right)}}} \quad (4-5)$$

based on Rohr empirical data. The term of $(\sigma^{0.1}/e^{-0.5072(t/d)})$ is applied only when the ratio of the plate thickness to hole diameter is less than one ($t/d < 1$). If $t/d > 1$, different empirical data are required to determine the discharge coefficient.

The non-linear mass reactance slope, S_m , (also discussed in Zorumski and Tester, Reference 1, pp. 15-16) was also determined using a Rohr empirical data base. The equation for this parameter can be expressed as

$$S_m = -0.000631 \frac{k}{\sigma^2} (\text{cm/sec})^{-1} \quad (4-6)$$

The negative slope value means that the mass reactance is reduced with increasing sound pressure (or particle velocity). Again, Equation (4-6) is true for the condition of $t/d < 1$.

An empirical approach is used by Rohr for wire mesh type linear face sheet impedance calculations. The DC flow resistance measurements are used to determine the acoustic resistance and mass reactance. When the wire mesh is bonded over a perforated plate, the blockage factor due to the bonding will be included to determine the liner impedance value. In addition, only half the end correction can be used to calculate the perforate plate impedance contribution because the end correction is eliminated on the perforate surface bonded to the wire mesh.

For the random noise spectrum, it is required to use the rms particle velocity for the overall frequency range, V_p , to solve for $Z/\rho c$ from Equation (4.1). The relationship between the individual particle velocity, V_{pf} and impedance, Z_f can be expressed as:

$$V_{pf} = \frac{P_f}{|Z_f|} \quad (4-7)$$

where V_{pf} and P_f are the rms values for the acoustic particle velocity and the sound pressure for frequency, f . Then the overall rms particle velocity, V_p , can be obtained from the definition of $V_p = (\sum (V_{pf})^2)^{1/2}$. As mentioned in Volume 2, Section 2.2.2.1, an iterative procedure that focuses on the values of $Z_f/\rho c$, V_{pf} , and V_p is required to solve for Equation (4-1).

4.2 Effective POA and Hole Diameter Estimate

4.2.1 Methods for Estimating Effective POA and Hole Diameter

For DC flow resistance, Equation (4-1) can be modified to a simple form as:

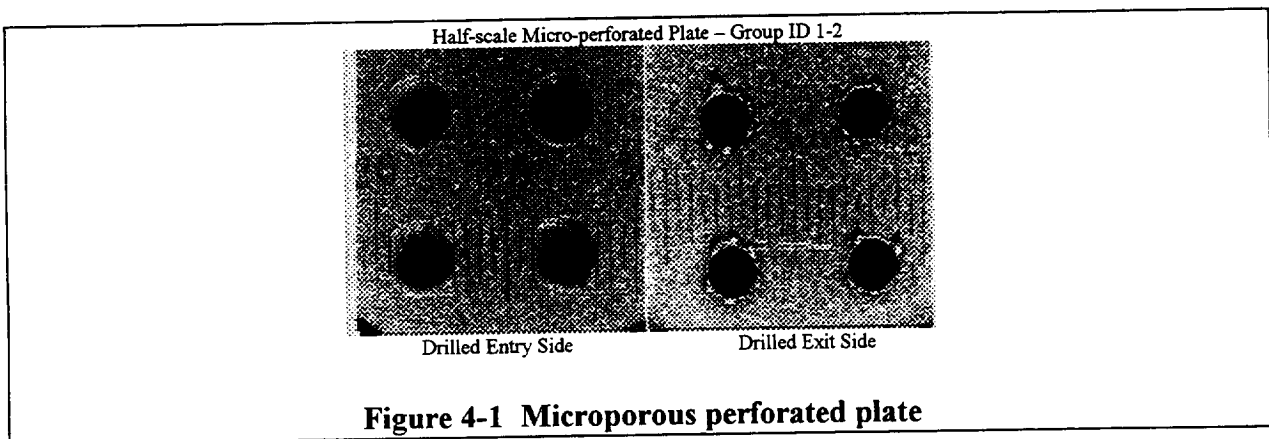
$$R(V) = R(0) + S \cdot V = \frac{32\mu t}{\sigma d^2} + S \cdot V \quad (4-8)$$

where $R(V)$ is the DC flow resistance at flow speed V , the intercept, $R(0)$, is the linear DC flow resistance defined in Volume 2 Equation (2-13), and S is the non-linear flow resistance slope defined by Equations (4-4) and (4-5). The relationship between open area ratio, σ , and average hole diameter, d , can be determined by the perforate hole pattern. It can be expressed as

$$\sigma = \frac{\pi \left(\frac{d}{2}\right)^2}{S_p^2} \quad (4-9)$$

where S_p is the hole spacing (center to center) and can be defined by using an average measurement value.

Based on Equations (4-4), (4-5), (4-8), and (4-9), one can determine the effective POA and effective hole diameter of a perforated plate using the DC flow resistance, plate thickness, and average hole spacing measurement results. An iterative procedure is used to determine the effective POA, σ , and effective hole diameter d . Inputs to the procedure are measured values for t and ρ , the measured DC flow coefficients, and the calculated value of S_p . Figure 4-1 shows a half-scale (1/2) sample (Group ID 1-2) of a laser drilled microporous perforated plate. The hole patterns on the left hand side represent the laser drilled entry side, and the patterns on the right hand side represent the laser drilled exit side.



Two observations were made from this figure. Note that a tapered hole exist (holes on the drilled entry side are larger than those on the drilled exit side). Secondly, the hole shape is not perfectly round. These two phenomena exist in all micro-perforated plate liners and results in hole size and POA measurement difficulties. However, using the DC flow resistance data that averages entry side and exit side data as well as the plate thickness and average hole spacing (center to center) measurements, one can easily calculate effective POA and effective hole diameter for an unbonded perforated skin. The same approach is not suitable for bonded acoustic panels because accurate DC flow measurements can only be performed from the unbonded perforated plate surface. A modified measurement technique derived from Rohr's empirical data base was used to determine the effective POA and hole diameter on bonded panels.

Table 4-1 shows the plate thickness, hole spacing, hole pattern and DC flow resistance data (intercept, slope, R(105) and NLF) of all perforate liner specimens used for normal incidence impedance measurements. The Sample ID specifies scale factor, Group ID, laser drilled direction, and bonding status. For example, for specimen 'S122F (1/2 skin)', the 'S' means sub-scale (F means full-scale). The first two digits '12' of 122 signifies a sample cut from Group ID 1-2 (see Table 2-1. The last digit '2' of 122 is an internal identification number used to identify normal incidence impedance tube samples and matches the test matrix (Appendix A).

Table 4-1 Perforate Plate Geometrical and DC Flow Resistance Measurements

Sample ID	Thickness	Spacing	Pattern	Intercept	Slope	R(105) ⁺⁺	NLF ^{**}
Perforated Liner	inch	inch		rayl	rayl/(cm/sec)	rayl	R(200)/R(20)
F113 (1/1 bond)	0.025	0.114	Stagger-60°	1.06	0.096	11.14	6.80
S122F(1/2 entry)	0.012	0.055	Square-90°	1.14	0.069	8.39	5.93
S122F(1/2 exit)	0.012	0.055	Square-90°	-0.44	0.093	9.33	12.79
S122F(1/2 avg)	0.012	0.055	Square-90°	0.35	0.081	8.86	8.40
S122 (1/2 bond)	0.012	0.055	Square-90°	1.20	0.083	9.92	6.22
S132F(1/5 entry)	0.005	0.022	Square-90°	2.07	0.064	8.83	4.45
S132F(1/5 exit)	0.005	0.022	Square-90°	1.57	0.070	8.88	5.23
S132F(1/5 avg)	0.005	0.022	Square-90°	1.82	0.067	8.86	4.82
S132 (1/5 bond)	0.005	0.022	Square-90°	2.99	0.091	12.53	4.40
F22 (1/1 bond)	0.032	0.127	Square-90°	0.36	0.053	5.93	7.72
S24F (1/2 entry)	0.016	0.063	Square-90°	0.73	0.038	4.72	5.59
S24F (1/2 exit)	0.016	0.063	Square-90°	-0.04	0.052	5.42	10.36
S24F (1/2 avg)	0.016	0.063	Square-90°	0.35	0.045	5.07	7.51
S24 (1/2 bond)	0.016	0.063	Square-90°	1.13	0.061	7.54	5.67
S26F (1/5 entry)	0.006	0.025	Square-90°	1.05	0.028	3.99	4.13
S26F (1/5 exit)	0.006	0.025	Square-90°	0.78	0.032	4.14	5.06
S26F (1/5 avg)	0.006	0.025	Square-90°	0.92	0.030	4.07	4.56
S26 (1/5 bond)	0.006	0.025	Square-90°	1.47	0.052	6.93	4.73
F32 (1/1 bond)	0.025	0.114	Stagger-60°	1.06	0.096	11.14	6.80
S34F (1/2 entry)	0.012	0.061	Square-90°	1.65	0.116	13.83	6.26
S34F (1/2 exit)	0.012	0.061	Square-90°	-0.88	0.177	17.71	12.98
S34F (1/2 avg)	0.012	0.061	Square-90°	0.39	0.147	15.77	8.95
S34 (1/2 bond)	0.012	0.061	Square-90°	1.66	0.134	15.73	6.56
S36F (1/5 entry)	0.005	0.024	Square-90°	1.79	0.049	6.94	4.18
S36F (1/5 exit)	0.005	0.024	Square-90°	1.47	0.053	7.04	4.77
S36F (1/5 avg)	0.005	0.024	Square-90°	1.63	0.051	6.99	4.46
S36 (1/5 bond)	0.005	0.024	Square-90°	3.44	0.078	11.65	3.81

⁺⁺ R(105) is measured flow resistance data at the flow velocity of 105 cm/sec

^{**} NLF, none linear factor, is the ratio of flow resistance data at flow velocity of 200 cm/sec to that at flow velocity of 20 cm/sec.

Inside the parenthesis, the scaling factor is specified on the left side, while the laser drilled direction and bonding status is specified on the right side. The unbonded perforated face sheets with the laser drilled entry side exposed are marked as 'entry' and the other side (laser drilled exit side) marked as 'exit'. The same face sheets bonded to a core blanket are marked as 'bond'. No DC flow measurement data was generated for the unbonded full-scale punched perforated liner specimens (F113, F22, and F32), because the POA and hole diameter of punched perforated

plates can be easily measured using a simple pin gauge (various sized pins used for hole size measurement).

For the skin, DC flow resistance is measured with flow traveling in both directions through the perforate plates. Average flow resistance data are used to determine the values of effective POA and effective hole diameter of given perforate sheet. Since both the intercept and non-linear slope are functions of POA and hole diameter, it is difficult to use regression analysis to solve Equation (4-8). For this reason, Rohr has developed a simplified method that uses the flow resistance slope (Equation (4-4)) to calculate effective POA and effective hole diameter (referred to as the 'Slope Method').

For bonded panels, the flow can only be accurately measured from the non-core bonded side. The 'Slope Method' can not be used to calculate an effective POA and effective hole diameter. Therefore, Rohr developed a method referred to as the 'R(105) Method' to handle bonded perforated samples. This method uses R(105), measured DC flow resistance data at 105cm/sec, to perform effective POA and effective hole diameter calculations. R(105) data, hole spacing, and thickness are used as input to Equation (4-8) to solve for the effective POA and effective hole diameter.

4.2.2 Perforated Liner Effective POA and Hole Diameter

Table 4-2 summarizes the results of effective POA and hole diameter on both unbonded and bonded perforated liner specimens. The input (measured data) is from Table 4-1. However, for the unbonded perforate skins, only averaged flow resistance data have been shown in Table 4-2 (with a slightly modified Sample ID). For example, in Table 4-1, sample S122F(1/2 avg.) is a 1/2-scale unbonded perforate specimen for which average DC flow resistance data is shown. In Table 4-2, this sample ID is changed from S122F(1/2 avg.) to S122F(1/2 skin).

The output (predicted data) in Table 4-2 is calculated using the 'Slope Method' for unbonded perforated skins, and the 'R(105) Method' for bonded specimens. In the 'Target' column, the POA values of unbonded perforate skins is higher than those of the bonded liner POA values. This difference is due to the adhesive bleeding into perforated holes, reducing and/or blocking some of the holes. In order to meet acoustic specifications of bonded panel, the blockage factor due to bonding must be carefully estimated to support the initial POA and hole diameter selection of unbonded skins.

For an unbonded perforate sheet, the 'Slope Method' is used for calculation of an effective POA and effective hole diameter. The method uses an iterative approach until the slope (SLP) in the output column matches that in the input column. The difference in intercept (INT) values between the input column and output column is ignored. Rohr's experience has shown that the method is accurate if the perforated plate has a large NLF (non-linear factor) and small intercept values. For this reason, ratios of t/d smaller than one are important because this assures a reasonably large NLF value for both full-scale and sub-scale perforated liners.

Table 4-2 Effective Hole Diameter and POA Calculation on Full-scale and Sub-scale Bonded Perforate Liners

Sample ID	Measured Data (Input)						Predicted Data (Output)						Target	
	THK inch	SP inch	PTN inch	INT Rayl	SLP Rayl	R(105) Rayl	DIA inch	POA %	INT Rayl	SLP Rayl	R(105) Rayl	NLF	DIA inch	POA %
F113 (1/1bond)	0.025	0.114	Stagger	1.06	0.096	11.14	.0358	8.94%	0.50	0.101	11.14	8.21	0.039	10.0%
S122F (1/2 skin)	0.012	0.055	Square	0.35	0.081	8.86	0.198	10.18%	0.69	0.081	9.16	7.30	0.020	10.4%
S122 (1/2 bond)	0.012	0.055	Square	1.20	0.083	9.92	0.194	9.78%	0.75	0.087	9.92	7.30	0.020	10.0%
S132F (1/5 skin)	0.005	0.022	Square	1.82	0.067	8.86	0.083	11.15%	1.50	0.067	8.49	5.23	0.008	10.4%
S132 (1/5 bond)	0.005	0.022	Square	2.99	0.091	12.53	0.082	9.13%	1.87	0.101	12.53	5.68	0.008	10.0%
F22 (1/1 bond)	0.032	0.127	Square	0.36	0.053	5.93	0.050	12.18%	0.24	0.054	5.93	8.36	0.051	12.0%
S24F (1/2 skin)	0.016	0.063	Square	0.35	0.045	5.07	0.259	13.32%	0.41	0.045	5.17	7.19	0.025	12.4%
S24 (1/2 bond)	0.016	0.063	Square	1.13	0.061	7.54	0.265	11.09%	0.47	0.067	7.54	7.66	0.025	12.0%
S26F (1/5 skin)	0.006	0.025	Square	0.92	0.030	4.07	0.115	16.62%	0.63	0.030	3.73	5.37	0.010	12.6%
S26 (1/5 bond)	0.006	0.025	Square	1.47	0.052	6.93	0.115	12.15%	0.86	0.058	6.93	6.17	0.010	12.0%
F32 (1/1 bond)	0.025	0.122	Stagger	1.51	0.116	13.69	0.365	8.11%	0.53	0.125	13.69	8.42	0.039	8.0%
S34F (1/2 skin)	0.012	0.061	Square	0.39	0.147	15.77	0.190	7.62%	1.00	0.147	16.43	7.71	0.020	8.4%
S34 (1/2 bond)	0.012	0.061	Square	1.66	0.134	15.73	0.192	7.79%	0.96	0.141	15.73	7.71	0.020	8.0%
S36F (1/5 skin)	0.005	0.024	Square	1.63	0.051	6.99	0.097	12.88%	0.94	0.051	6.32	5.68	0.008	8.7%
S36 (1/5 bond)	0.005	0.024	Square	3.44	0.078	11.65	0.095	9.46%	1.35	0.098	11.65	6.34	0.008	8.0%

Method 1: Match Slope (Average entry & exit measured data)

THK: Perforate plate thickness

SP : Hole spacing; PTN: Perforate pattern

INT: DC flow resistance data intercept

SLP: DC flow resistance data slope

Method 2: Match R(105); used for bonded panels

DIA: Average hole diameter

POA: Perforate skin open area

R(V) = INT + SLP * V; R(105) = INT + SLP * 105

NLF = R(200)/R(20)

For the bonded perforate samples, the 'R(105) Method' is used. DC flow resistance data is measured from the plate side of the assembly. In order to calculate the effective POA and effective hole diameter, an iterative approach is used to force the value of R(105) in the output column to match that of the input column. While, the intercept and slope may not be well matched, effective POA and hole diameter predictions are good based on Rohr's experience. At Rohr, the value of R(105) is used as a gauge of an acoustic liner property. As a result, an extensive data base has been generated which allows the engineer to develop a semi-empirical model using the 'R(105) Method' to estimate liner acoustic properties.

4.3 Normal Incidence Impedance Measurement Data

4.3.1 Data Analysis and Evaluation Approach

Three sets of acoustic liner specimens are used to perform normal incidence impedance evaluation. The first set consists of SDOF perforated plate liners, the second set SDOF linear liners, and the third set DDOF linear liners. In-tube impedance measurement data obtained from Rohr's 10 cm (174 - 1524 Hz), 3cm (824 - 6224 Hz), and 1.5 cm (2762 - 13472 Hz) impedance measuring systems (see Section 3.3) are used to compare with impedance prediction results. Input parameters consisting of sound pressure level, temperature and static pressure are provided during impedance measurements.

The liner core depth, plate thickness, hole pattern and spacing, R(105) and NLF are obtained from geometrical and DC flow resistance measurements. The effective POA and effective hole diameter of the unbonded and bonded perforate plate liners are derived from the 'Slope Method' and 'R(105) Method' respectfully. Rohr's SDOF analytical prediction model (described by Equations (4-1) through (4-7)) is used for impedance predictions of the SDOF perforate and wire mesh type linear liners.

A Rohr-developed DDOF (Double-Degree-Of-Freedom) liner impedance analytical prediction model is used for DDOF linear liner impedance predictions. Figure 4-2 is a simple DDOF acoustic liner sketch illustrating the cavity dimensions. The wave solution in the cavity is assumed to be one-dimensional in the cavity height direction, with origins at the backplate in lower Cavity 1 and at the septum in upper Cavity 2.

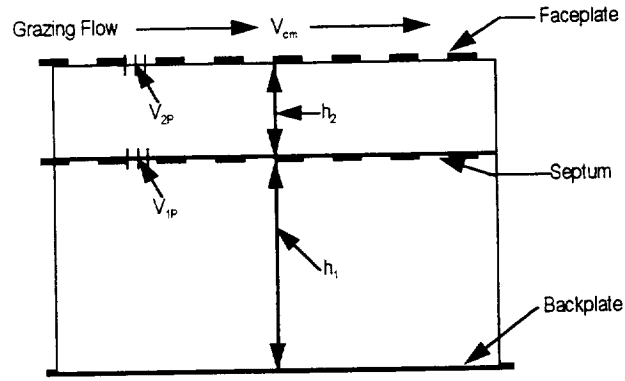


Figure 4-2 DDOF Acoustic Liner

The general analytical equation that is derived from Zorumski and Tester, Reference 1 (Equation 45, p. 34) can be expressed as follows:

$$\frac{Z_f}{\rho c} = R + iX = \frac{Z_{2f}}{\rho c} + \frac{1}{\left(\frac{Z_{1f}}{\rho c} - i \cot(kh_2)\right) \sin(kh_2)^2} \quad (4-9)$$

where, $Z_f/\rho c$ is the DDOF liner total impedance. Subscript '1' represents the parameters between the septum-to-back plate area and subscript '2' represents parameters from faceplate-to-septum area. For example, the faceplate $Z_{2f}/\rho c$ represents the liner impedance of a face sheet plate with core depth h_2 and $Z_{1f}/\rho c$ represents the liner impedance of the septum with core depth h_1 . Replacing Equation (4-1) with Figure 4-2 notations, yields:

$$\begin{aligned} \frac{Z_{2f}}{\rho c} = R_2 + iX_2 = & R_{20} + R_{20f} + S_{2r}V_{2p} + R_{cm}(V_{cm}) \\ & + i[X_{2m} + S_{2m}V_{2p} + X_{2em}(V_{cm}) - \cot(kh_2)] \end{aligned} \quad (4-10)$$

and

$$\frac{Z_{1f}}{\rho c} = R_1 + iX_1 = R_{10} + R_{10f} + S_{1r}V_{1p} + i[X_{1m} + S_{1m}V_{1p} + X_{1em}(0) - \cot(kh_1)] \quad (4-11)$$

It is assumed that Mach number effects do not apply to the septum. Equation 4-12 eliminates the Mach number related resistance and reactance terms. The relationship between V_{1pf} and V_{2pf} can be expressed as:

$$V_{2pf} = V_{1pf} \left| \cos(kh_2) + i \frac{Z_{1f}}{\rho c} \sin(kh_2) \right| \quad (4-12)$$

The overall rms particle velocities V_{1p} and V_{2p} can be calculated from the definition of $V_{1p} = (\sum (V_{1pf})^2)^{1/2}$ and $V_{2p} = (\sum (V_{2pf})^2)^{1/2}$, respectively. Although the iteration procedure is more complicated than that of the SDOF acoustic analytical model, it still converges quite rapidly.

4.3.2 SDOF Perforate Plate Liner Impedance Data Analysis

Fifteen perforate liner configurations were evaluated using normal incidence impedance measuring systems. Table 4-3 lists all the key input and output parameters for these liner configurations. These include liner plate thickness and hole spacing, effective hole diameter and POA, DC flow resistance data, overall sound pressure levels, and the average mass reactance values at different frequency ranges.

Table 4-3 Acoustic Parameters of Perforated Liner Samples

Impedance Test Sample ID	Perforated plated			Discharge Coefficient	DC Flow Resistance			In-tube OASPL (dB)			Mass Reactance Per Wave Number (CGS Units)					
	THK	DIA	POA		Core	INT	SLP	10 cm	3 cm	1.5 cm	Intercept (Average data at 0 cm/s)			Slope k/cm		
	inch	inch	inch		inch	Rayl	Rayl-cm/sec	Tube	tube	Tube	174-1524 Hz	824-6224 Hz	2672-13472 Hz			
Perforate Liner																
F113 (1/1Bond)	0.025	0.036	8.94%	1.0	0.502	0.101	144.5	141.9	--	1.637	1.518	--	--	-0.00259		
S122F (1/2 skin)	0.012	0.020	10.18%	0.5	0.691	0.081	--	143.8	129.9	--	0.723	0.690	0.690	-0.00200		
S122 (1/2 bond)	0.012	0.019	9.78%	0.5	0.749	0.087	--	143.7	130.8	--	0.749	0.714	0.714	-0.00216		
S132F (1/5 skin)	0.005	0.008	11.15%	0.5**	1.499	0.067	--	143.8	130.2	--	0.305	0.290	0.290	-0.00167		
S132 (1/5 bond)	0.005	0.008	9.13%	0.5**	1.873	0.101	--	143.9	130.7	--	0.376	0.359	0.359	-0.00248		
F22 (1/1 bond)	0.032	0.050	12.15%	1.0	0.242	0.054	144.4	141.4	--	1.515	1.426	--	--	-0.00140		
S24F (1/2 skin)	0.016	0.026	13.32%	0.5	0.410	0.045	--	143.2	129.7	--	0.693	0.667	0.667	-0.00117		
S24 (1/2 bond)	0.016	0.027	11.09%	0.5	0.472	0.067	--	143.4	130.4	--	0.853	0.821	0.821	-0.00168		
S26F (1/5 skin)	0.006	0.012	16.62%	0.2	0.627	0.030	--	145.7	136.3	--	0.246	0.233	0.233	-0.00075		
S26 (1/5 bond)	0.006	0.012	12.15%	0.2	0.858	0.058	--	145.9	136.2	--	0.347	0.328	0.328	-0.00183		
F32 (1/1 bond)	0.025	0.036	8.11%	1.0	0.532	0.125	144.1	142.4	--	1.831	1.698	--	--	-0.00315		
S34F (1/2 skin)	0.012	0.019	7.62%	0.5	1.002	0.147	--	144.1	130.3	--	0.969	0.923	0.923	-0.00357		
S34 (1/2 bond)	0.012	0.019	7.79%	0.5	0.959	0.141	--	144.3	130.7	--	0.951	0.906	0.906	-0.00341		
S36F (1/5 skin)	0.005	0.010	12.88%	0.2	0.944	0.051	--	145.8	136.2	--	0.279	0.279	0.279	-0.00125		
S36 (1/5 bond)	0.005	0.010	9.46%	0.2	1.346	0.098	--	145.9	136.1	--	0.387	0.366	0.366	-0.00231		

** 0.5 inch core depth used to support GE flow duct impedance measurements

The comparison between impedance predictions and data measurements are shown in Figures 4-3 through 4-17. In each figure, two sets of data are presented. For example, the full-scale specimens show the data obtained from 10 cm (174 to 1524 Hz) and 3 cm (824 to 6224 Hz) impedance measuring systems as well as the prediction results. For the sub-scale specimens, they show the data obtained from 3 cm and 1.5 cm (2762 to 13472 Hz) impedance measuring systems. The symbols represent the measured data and solid lines represent the predicted results.

Figure 4-3

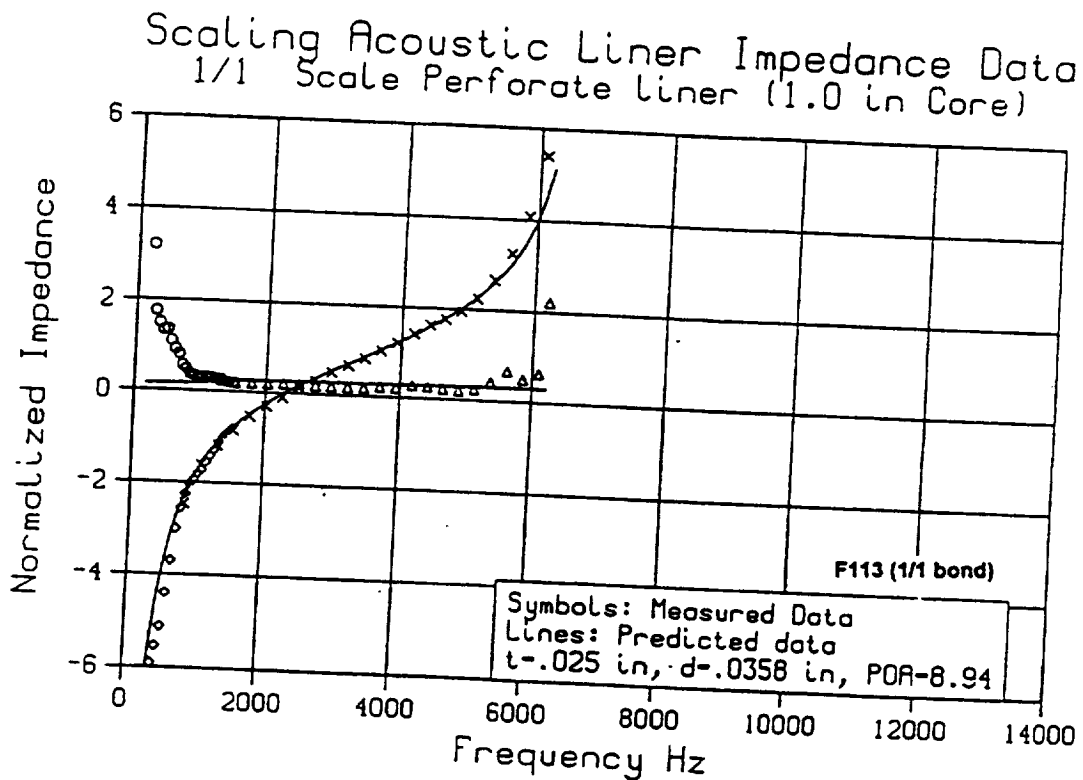


Figure 4-4

Scaling Acoustic Liner Impedance Data
1/2 Scale Perforate Face (0.5 in Core)

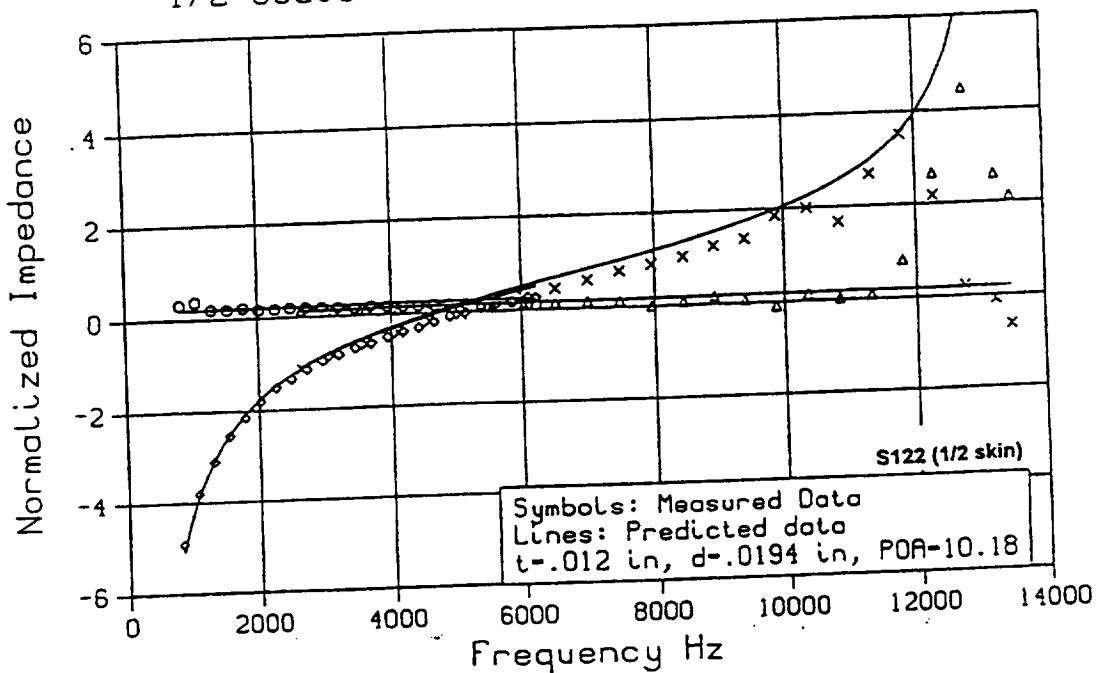


Figure 4-5

Scaling Acoustic Liner Impedance Data
1/2 Scale Perforate Liner (0.5 in Core)

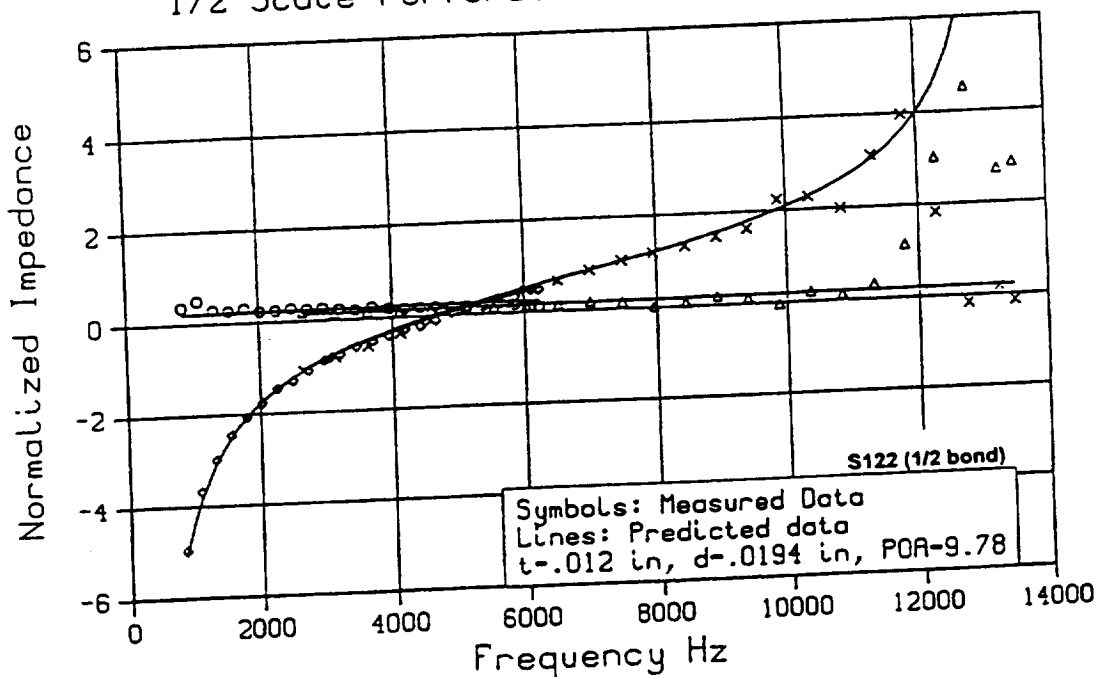


Figure 4-6

Scaling Acoustic Liner Impedance Data
1/5 Scale Perforate Face (0.5 in Core)

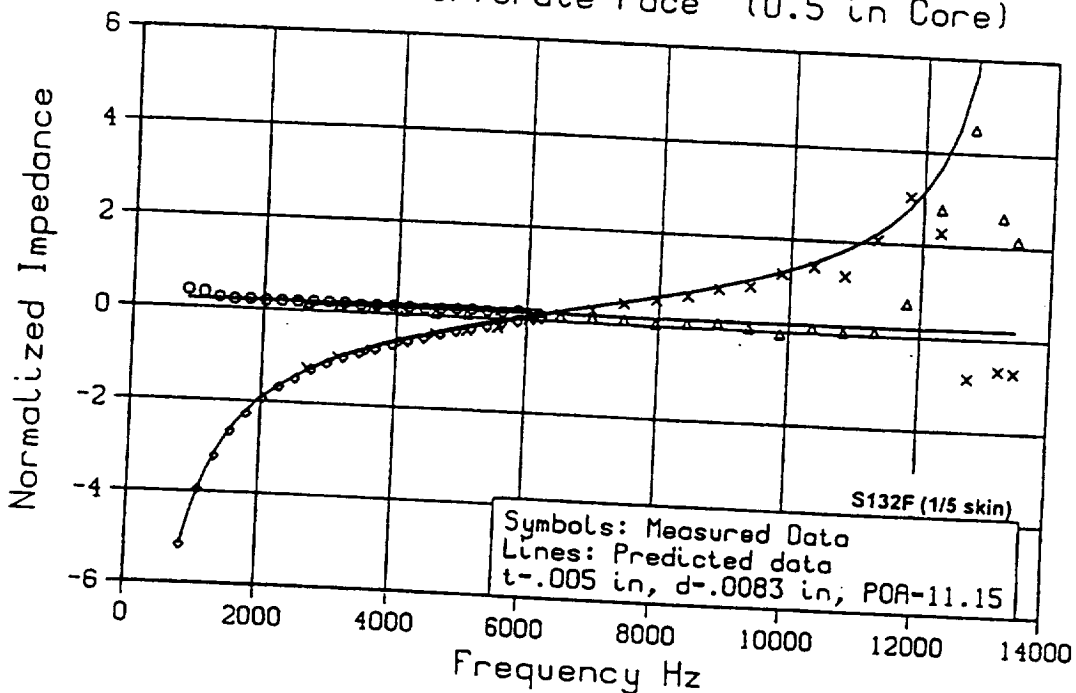


Figure 4-7

Scaling Acoustic Liner Impedance Data
1/5 Scale Perforate Liner (0.5 in Core)

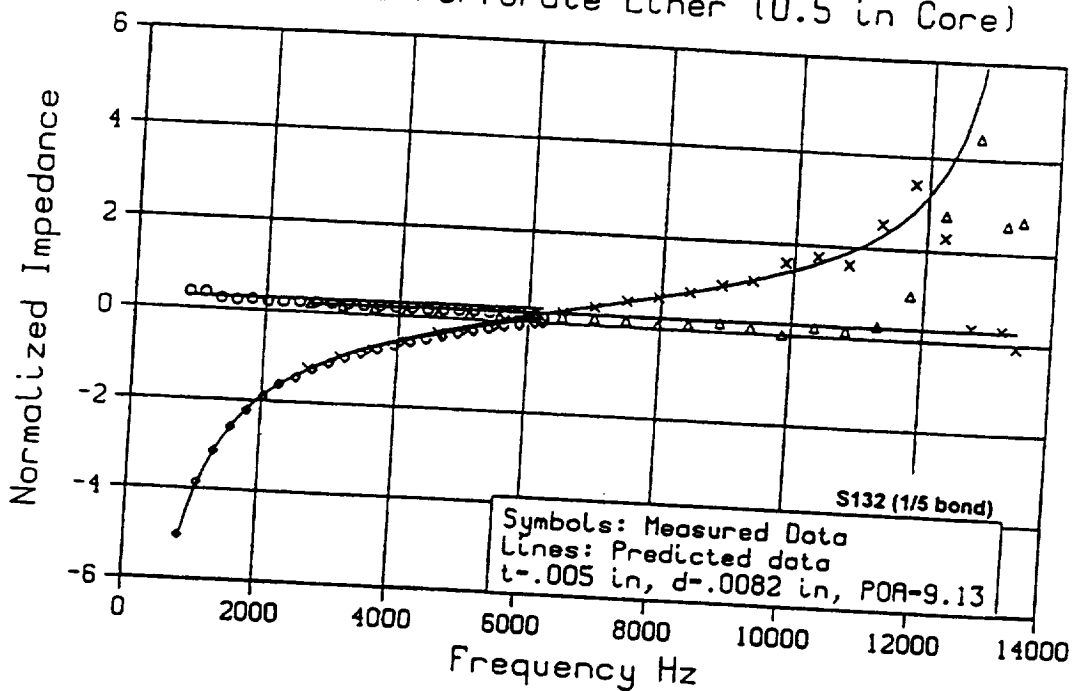


Figure 4-8

Scaling Acoustic Liner Impedance Data
1/1 Scale Perforate Liner (1.0 in Core)

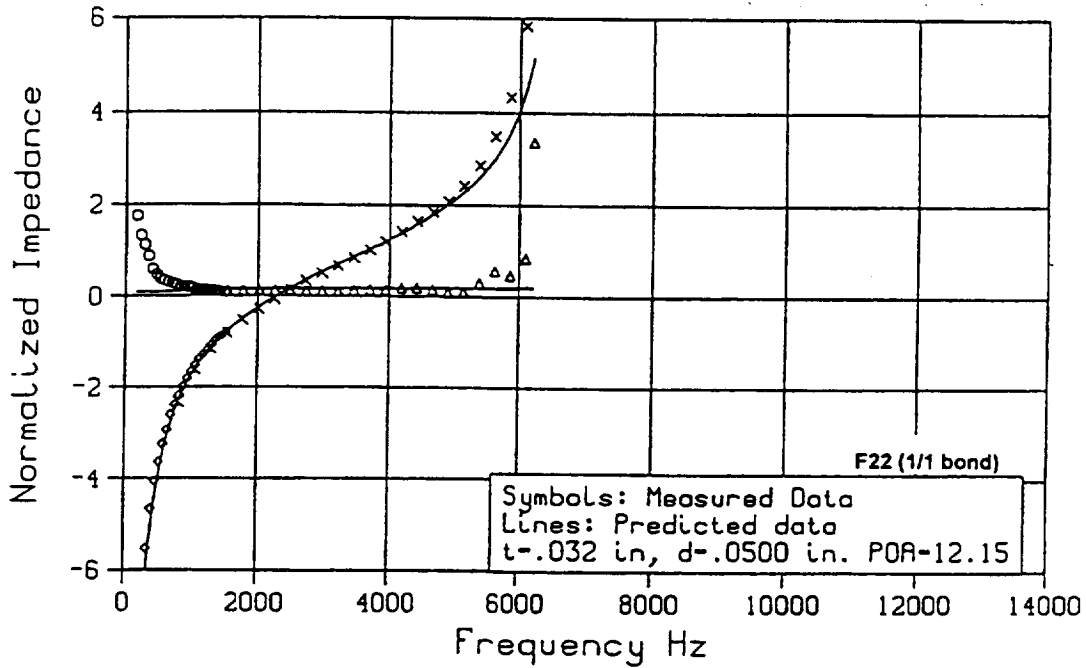


Figure 4-9

Scaling Acoustic Liner Impedance Data
1/2 Scale Perforate Face (0.5 in Core)

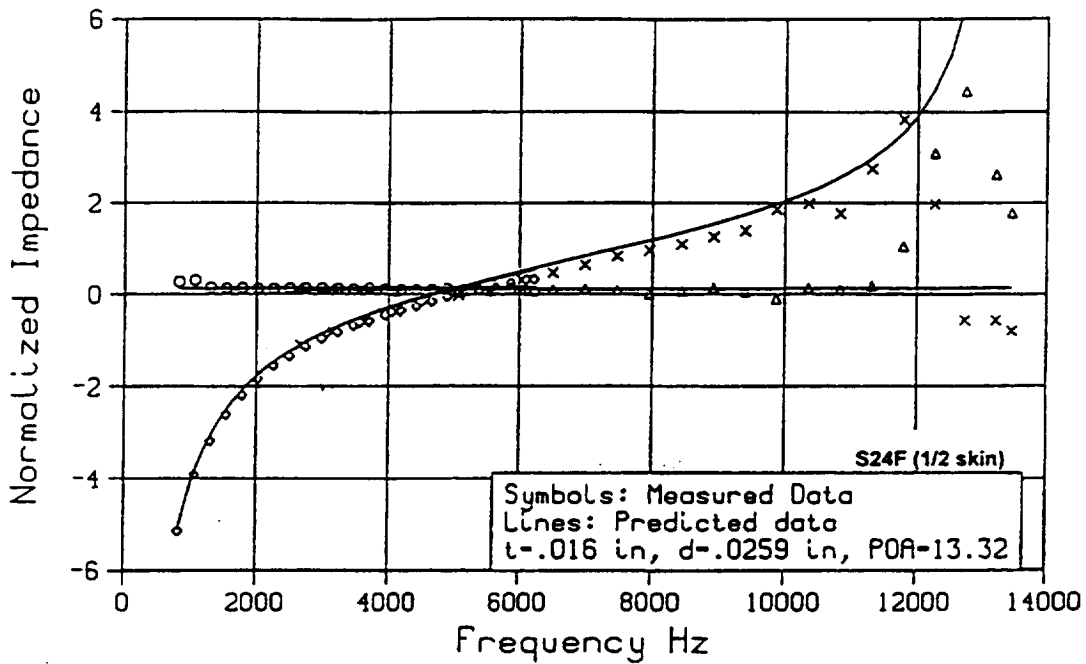


Figure 4-10

Scaling Acoustic Liner Impedance Data
1/2 Scale Perforate Liner (0.5 in Core)

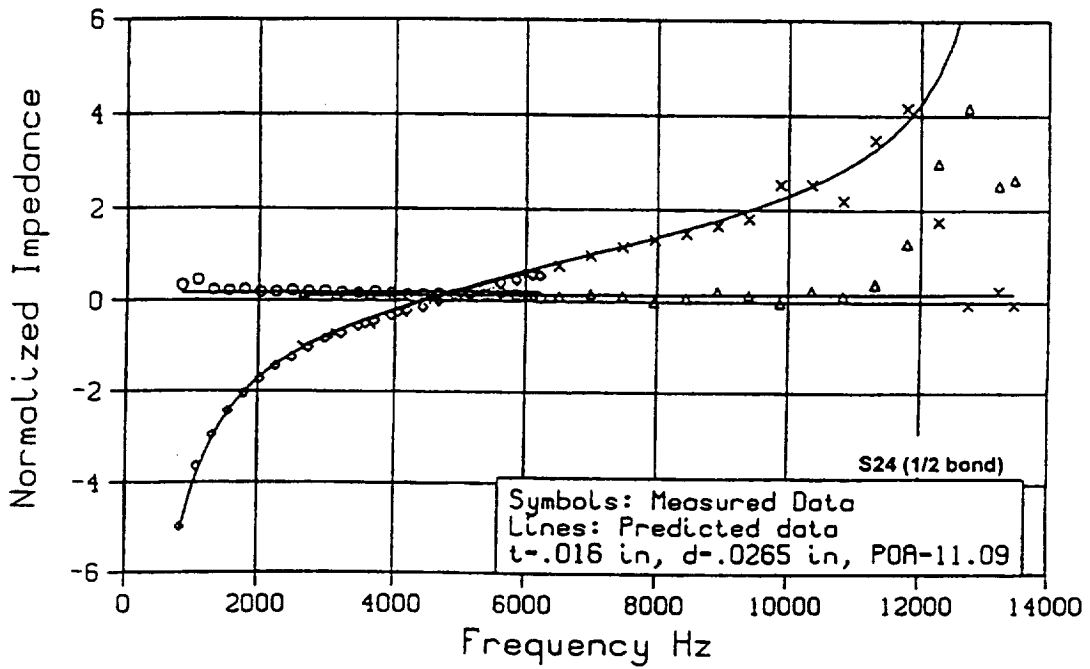


Figure 4-11

Scaling Acoustic Liner Impedance Data
1/5 Scale Perforate Face (0.2 in Core)

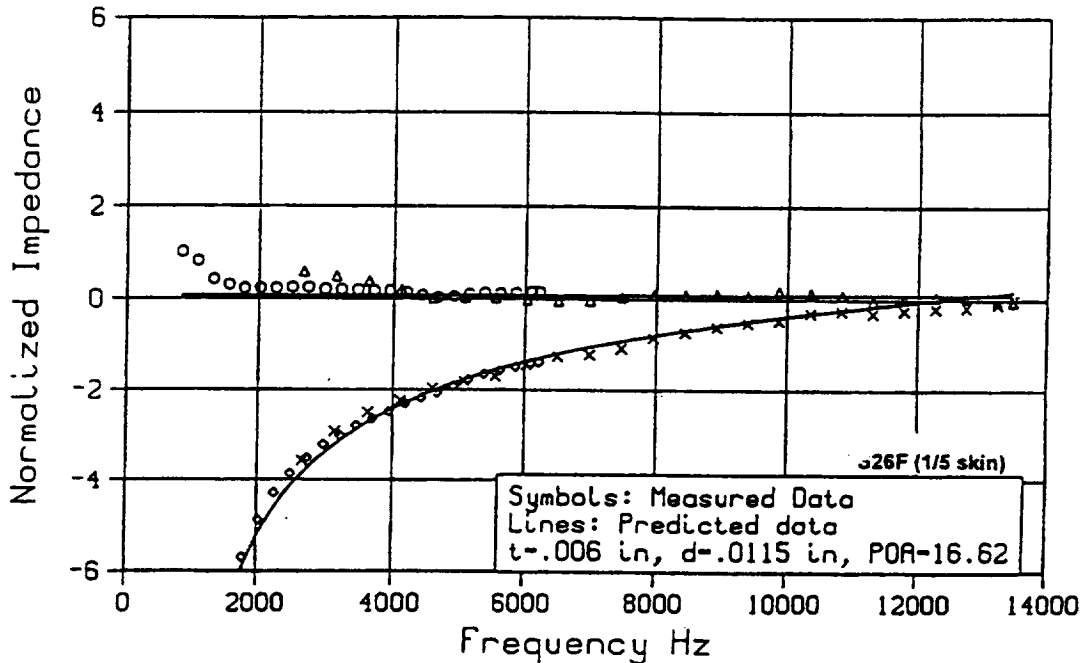


Figure 4-12

Scaling Acoustic Liner Impedance Data
1/5 Scale Perforate Liner (0.2 in Core)

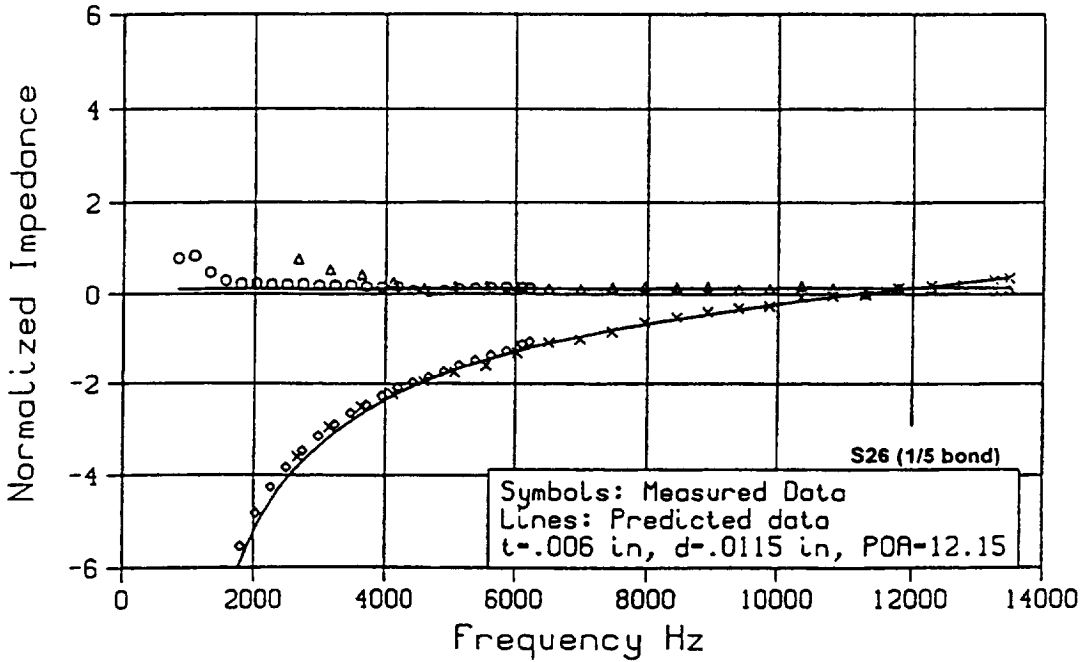


Figure 4-13

Scaling Acoustic Liner Impedance Data
1/1 Scale Perforate Liner (1.0 in Core)

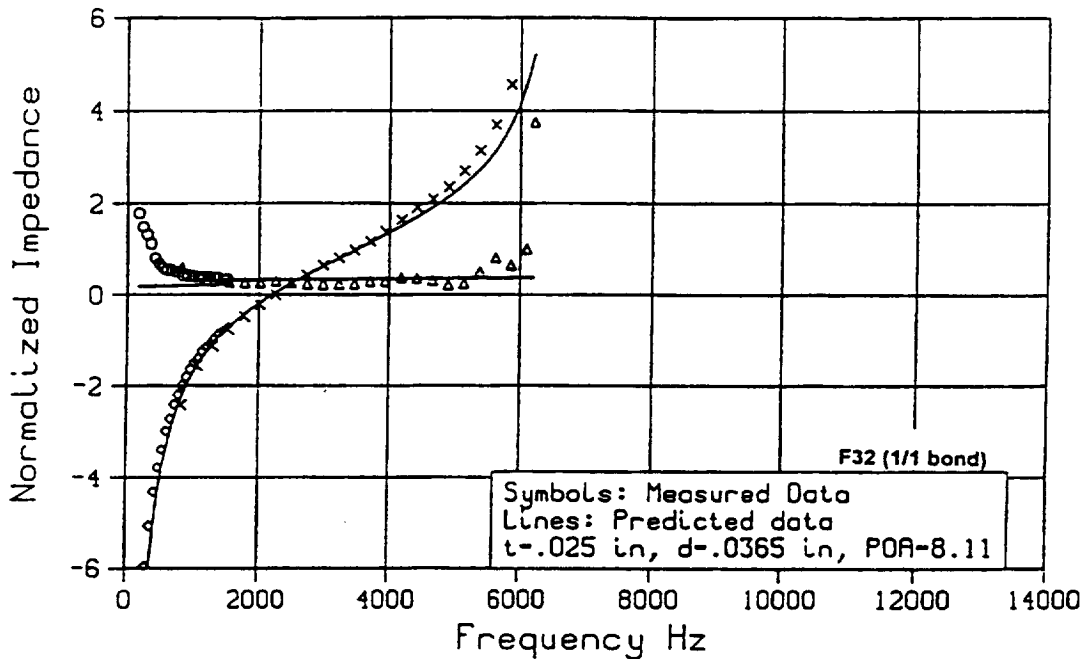


Figure 4-14

Scaling Acoustic Liner Impedance Data
1/2 Scale Perforate Face (0.5 in core)

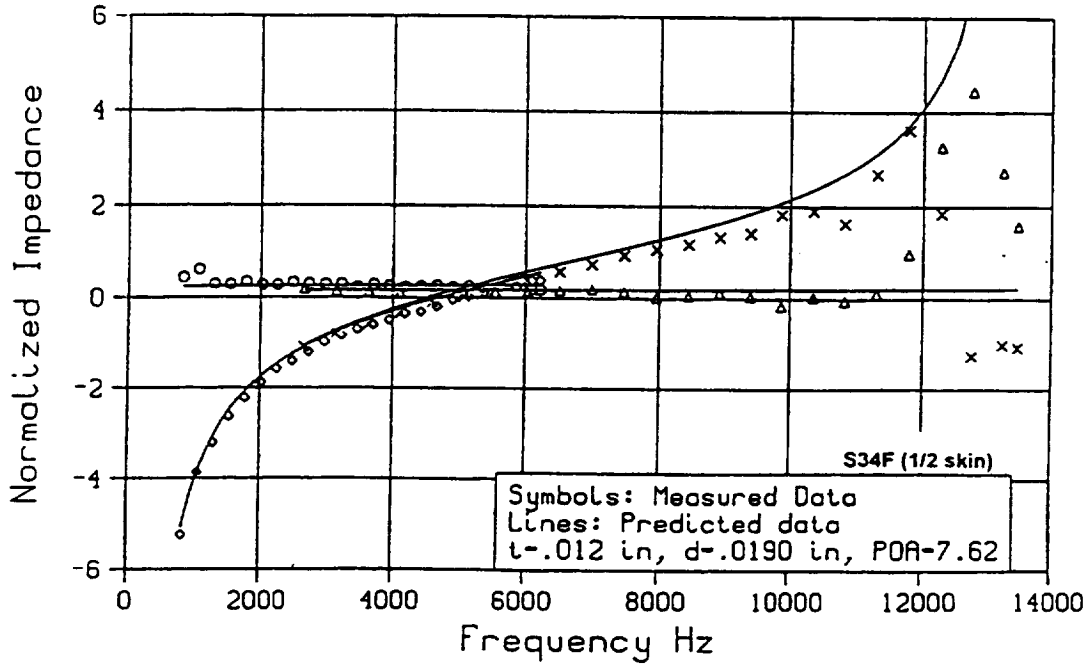


Figure 4-15

Scaling Acoustic Liner Impedance Data
1/2 Scale Perforate Liner (0.5 in core)

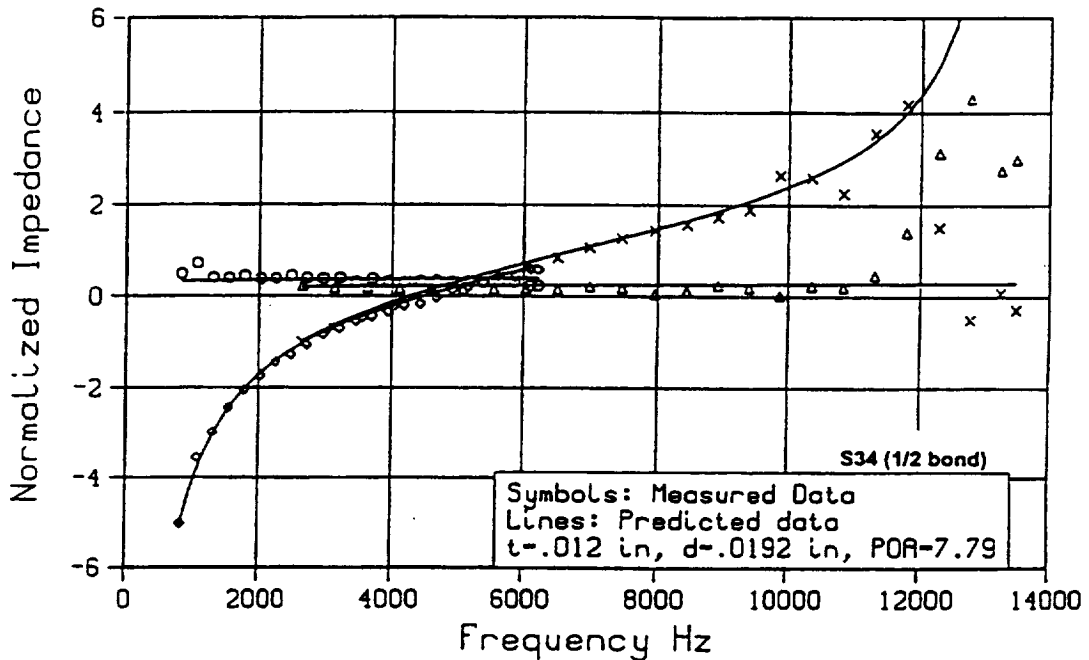


Figure 4-16

Scaling Acoustic Liner Impedance Data
1/5 Scale Perforate Face (0.2 in Core)

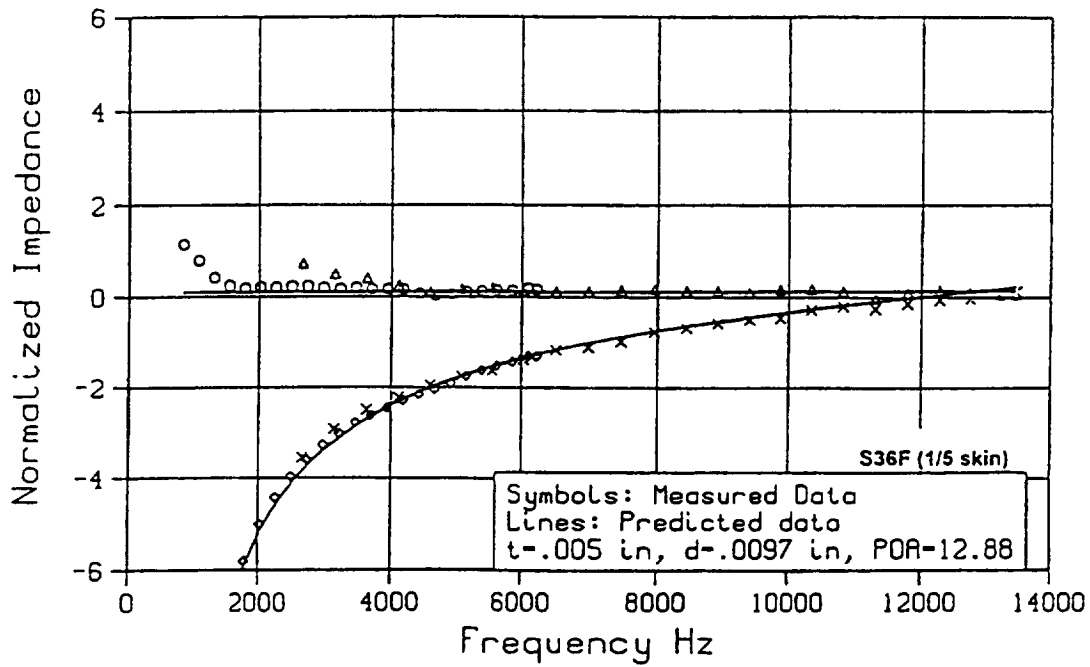
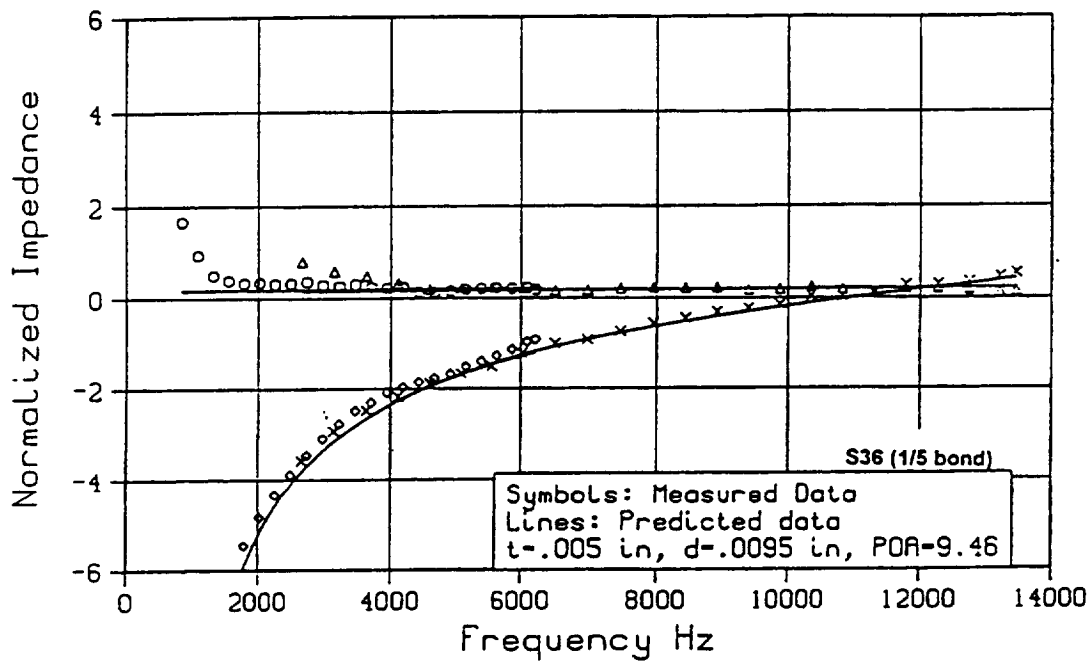


Figure 4-17

Scaling Acoustic Liner Impedance Data
1/5 Scale Perforate Liner (0.2 in Core)



Several key findings that are important for treatment scaling are discussed below.

1. For full-scale specimens, the two sets of data have sound pressure levels that are very close during the measurements (see Table 4-3). As a result, both resistance and reactance curves overlap in the transition area (824 Hz to 1524 Hz) between two data sets. For sub-scale specimens, the sound pressure levels between the two sets of data are quite different. This creates slightly different resistance levels between the two data, but no significant deviation in the reactance data.
2. Excellent agreement exists between impedance predictions and data measurements for all fifteen full- and sub-scale liner configurations. The measured data were generated from three different size impedance measuring systems that cover frequency ranges from 174 to 13472 Hz. However, some data scattering is observed at frequencies above 12000 Hz for all of the 0.5 inch core depth liner specimens (Samples S122F, S122, S132F, 132, S24F, S24, S34F, and S34). This is caused by the singularity point created by the $\cot(kh)$ term at frequencies in the 13500 to 13700 Hz range. When a frequency approaches the singularity point, the value of $\cot(kh)$ approaches infinity and creates measurement difficulties. However, the scattering above 12000 Hz seems to yield a similar pattern in all 0.5 inch core specimens. For example, the reactance value decreases for frequencies that exceed 12000 Hz and a peak resistance value occurs at 12750 Hz. It is possible to predict similar results (or at least trends) by adding a small imaginary number to the wave number 'k' (see Zorumski and Tester, Reference 1, Equation 44, p. 33) to solve Equation (4-1). Since this exceeded the study scope, further exploration was not made.
3. The resistance level obtained from the 10 cm impedance measuring system is quite high at the low frequency end (samples F113, F22, and F32). Similar phenomena occur on 0.2 inch core depth liners (S26F, S26, S36F, and S36) using the 3 cm measuring system, but the deviation scale is much smaller. The phenomena that show high resistance levels at the low frequency end occur as the reactance approaches large negative values. When the core depth is increased from 0.2 inch to 0.5 inch for the 1/5-scale samples (S132F and S132), they possess less negative reactance levels than the other 1/5-scale samples at the low frequency end. As a result, the abnormally high resistance levels on these two test samples are minimized. No definite explanation exists as the cause of this phenomena, but the apparatus limitations probably play an important role.
4. The mass reactance constant is referred to as the intercept of the mass reactance per wave number. Table 4-3 shows that the mass reactance constant in the lower frequency range is less than that at higher frequencies. For example, the mass reactance constant for 10 cm tube data (174 - 1424 Hz) is less than that for 3 cm tube data (824 - 6224 Hz) and the 3 cm tube data is less than the 1.5 cm tube data (2627 - 13472 Hz). Since predictions and data measurements correlate well in all frequency ranges, the size of the impedance measuring system is not responsible for the change in the mass reactance constant. It is noted that the mass reactance constant definition is derived from a traditional Helmholtz principle. As discussed in Volume 2, Section 4.1.3, both the Helmholtz and Poiseuille principles are approximations of Crandall's model for calculating perforate plate frequency

dependent acoustic impedance. In these approximate approaches, the mass reactance per wave number is a constant. This is not the case when the exact solution is used to solve for Crandall's model. A similar argument also can be made for the acoustic resistance. Since, the non-linear term (function of particle velocity) normally dominates the total acoustic resistance, the change in the resistance constant (frequency dependent) is small and difficult to observe. Nevertheless, the exact solution of Crandall's model should be used for scale treatment studies.

Empirical factors are used to calculate the non-linear resistance slope and non-linear mass reactance slope for a perforate liner. For the non-linear acoustic resistance, the empirical factors are the orifice discharge coefficient and the constant between acoustic non-linear resistance slope and the DC flow resistance slope. As discussed in Volume 2, Section 4.2.1, it is difficult to determine the discharge coefficient accurately using existing theory. The empirical factor described in Equation (4-5) is used for this data analysis. The constant between the acoustic resistance and DC flow resistance from Equation 4-3 is also modified. An empirical value of 1.336541 (based on Rohr experience) is used to replace the number 1.14 or 1.2 used in other impedance method models (See Section 4.1). The negative mass reactance slope described in Equation (4-6) resolves the mass reactance overprediction problem, especially for high sound pressure spectral levels.

By using an effective POA and effective hole diameter as input, as well as the exact solution for Crandall's model, and introducing empirical factors for non-linear resistance and reactance, an improvement to the impedance prediction accuracy discussed in Volume Section 4.3 is realized. In addition, by choosing the plate thickness to hole diameter ratio, t/d , less than one, the same acoustic impedance model can be used to predict both full- and sub-scale liner impedance. This significantly simplifies the complexity needed to simulate a full-scale liner acoustic impedance using sub-scale acoustic treatment. However, further studies are required to carefully examine grazing flow effects, especially at high frequency conditions.

4.3.3 SDOF and DDOF Linear Liner Impedance Data Analysis

Four SDOF and two DDOF linear liner configurations were evaluated using normal incidence impedance measuring systems. Tables 4-4 and 4-5 list all the key input and output parameters for these six liner configurations. These include wire mesh DC flow resistance data, perforate plate thickness and hole spacing, effective hole diameter and POA, bonded liner DC flow resistance data, overall sound pressure levels, and the average mass reactance values at different frequency ranges. The comparison between impedance predictions and data measurements are shown in Figures 4-18 through 4-23. The data plot format is identical to the perforated liners discussed in the previous section (4.3.2). However, no 1/2-scale acoustic liners are included in the linear liner study.

Table 4-4 Acoustic Parameters for SDOF & DDOF Linear Liner Samples (1)

SDOF	Wire mesh Resistance	Perforate Skin Dimension				Measured DC Flow Resistance				Target	
		THK	DIA	POA**	Core	Intercept	Slope	R(105)	NLF	DC Flow Resistance	NLF
Linear Liner	R(105) - Rayl / NLF	inch	inch		Inch	Rayl	Rayl*sec/cm	Rayl		Rayl	
Sample ID											
F43 (1/1 bond)	32.1 / 1.14	0.025	0.050	32.0%	1.0	63.18	0.181	82.17	1.49	90.0	1.5
S45 (1/5 bond)	59.1 / 1.11	NA	NA	NA	0.2	75.02	0.065	81.89	1.15	90.0	1.2
F53 (1/1 bond)	22.0 / 1.15	0.025	0.050	32.0%	1.0	43.90	0.125	578.06	1.49	60.0	1.5
S55 (1/5 bond)	36.0 / 1.13	NA	NA	NA	0.2	43.03	0.048	48.09	1.20	60.0	1.2
DDOF											
Linear Liner	Wire mesh	Perforate Skin Dimension				Measured DC Flow Resistance				Target	
Sample ID	R(105) - Rayl / NLF	THK	DIA	POA**	Core	Intercept	Slope	R(105)	NLF	DC Flow Resistance	NLF
		inch	inch		inch	Rayl	Rayl*sec/cm	Rayl		Rayl	
F613 (1/1 bond) - Face	14.8 / 1.21	0.025	0.050	32.0%	0.90	41.86	0.136	56.14	1.55	40.0	1.5
F613 - Septum	25.9 / 1.15	0.025	0.050	26.0%	1.50	73.44	0.339	109.03	1.76	100.	1.7
S623(1/5 bond) - Face	29.4 / 1.14	NA	NA	NA	0.18	38.77	0.044	43.35	1.20	40.0	1.2
S623 - Septum	52.2 / 1.12	NA	NA	NA	0.30	98.45	0.161	115.31	1.28	90.0	1.3

** This is installed POA (bonded with mesh and core). The bare perforated plate POA is 34 % initially.

Table 4-5 Acoustic Parameters for SDOF & DDOF Linear Liner Samples (2)

SDOF Linear Liner	In-tube OASPL			Mass Reactance Per Wave Number (CGS Units)			
	10.0 cm tube	3.0 cm tube	1.5 cm tube	Intercept (Average data at 0 cm/s)			Slope
Sample ID	dB	dB	dB	174-1524 Hz	824-6224 Hz	2672-13472 Hz	
F43 (1/1 bond)[145.7	145.7	--	0.787	0.764	--	-0.00007
S45 (1/5 bond)	--	147.4	137.5		0.317	0.317	-0.00000
F53 (1/1 bond)	145.4	145.3	--	0.669	0.669	--	-0.00007
S55 (1/5 bond)	--	146.9	137.1	--	0.215	0.215	-0.00000
DDOF Linear Liner	In-tube OASPL			Mass Reactance Per Wave Number (CGS Units)			
	10.0 cm tube	3.0 cm tube	1.5 cm tube	Intercept (Average data at 0 cm/s)			Slope
Sample ID	dB	dB	dB	174-1524 Hz	824-6224 Hz	2672-13472 Hz	
F613 (1/1 bond) - Face	144.2	145.5	--	0.631	0.611	--	-0.00007
F613 - Septum	--	--	--	0.827	0.803	--	-0.00010
S623 (1/5 bond) - Face	--	146.85	136.77	--	0.208	0.208	-0.00000
S623 - Septum	--	--	--	--	0.385	0.385	-0.00000

Figure 4-18

Scaling Acoustic Liner Impedance Data
1/1 Scale Linear Liner (1.0 in Core)

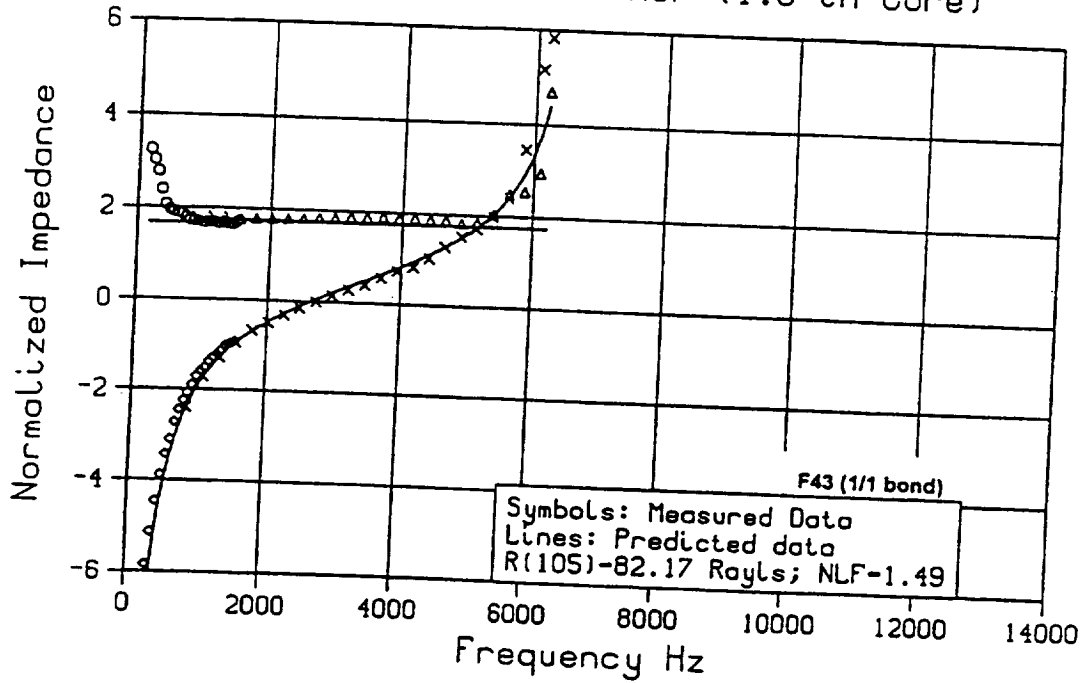


Figure 4-19

Scaling Acoustic Liner Impedance Data
1/5 Scale Linear Liner (0.2 in Core)

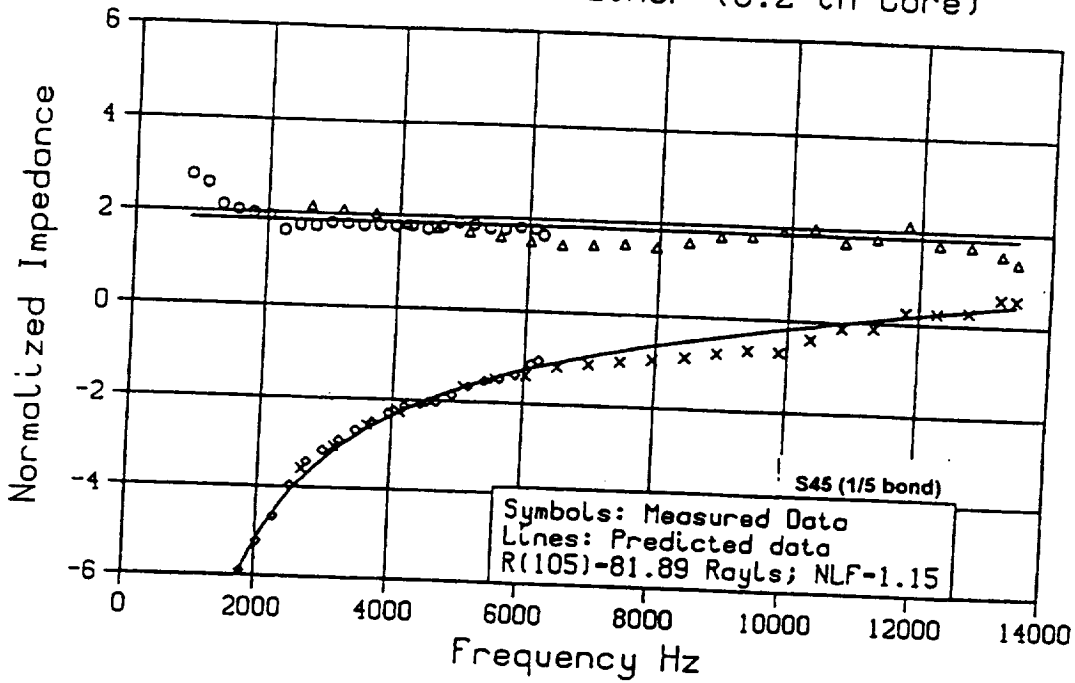


Figure 4-20

Scaling Acoustic Liner Impedance Data
1/1 Scale Linear Liner (1.0 in Core)

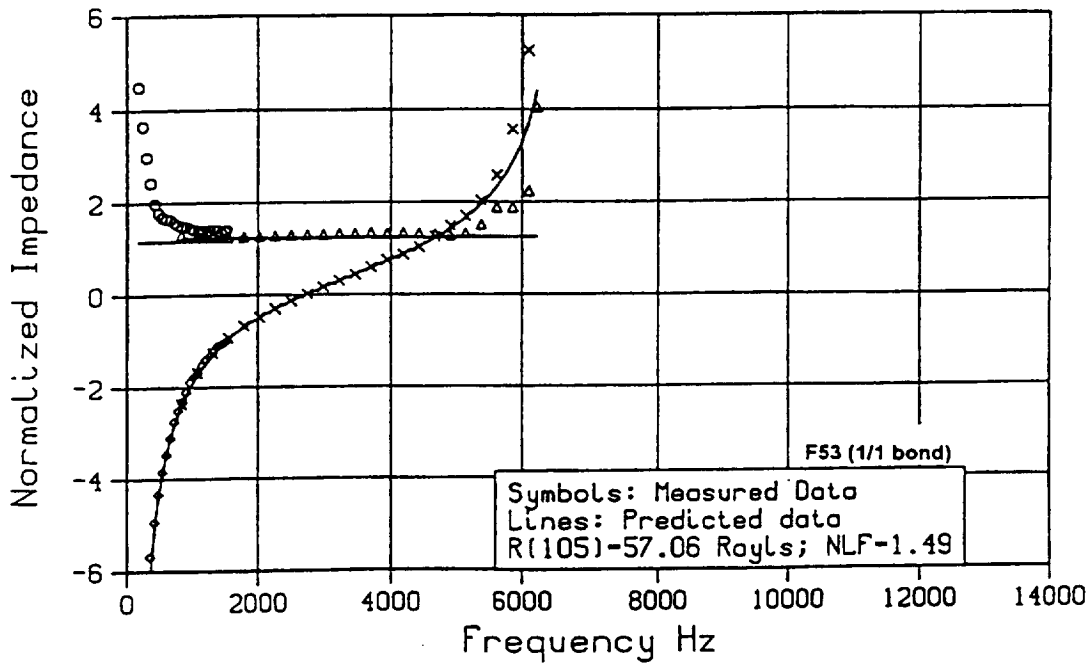


Figure 4-21

Scaling Acoustic Liner Impedance Data
1/5 Scale Linear Liner (0.2 in Core)

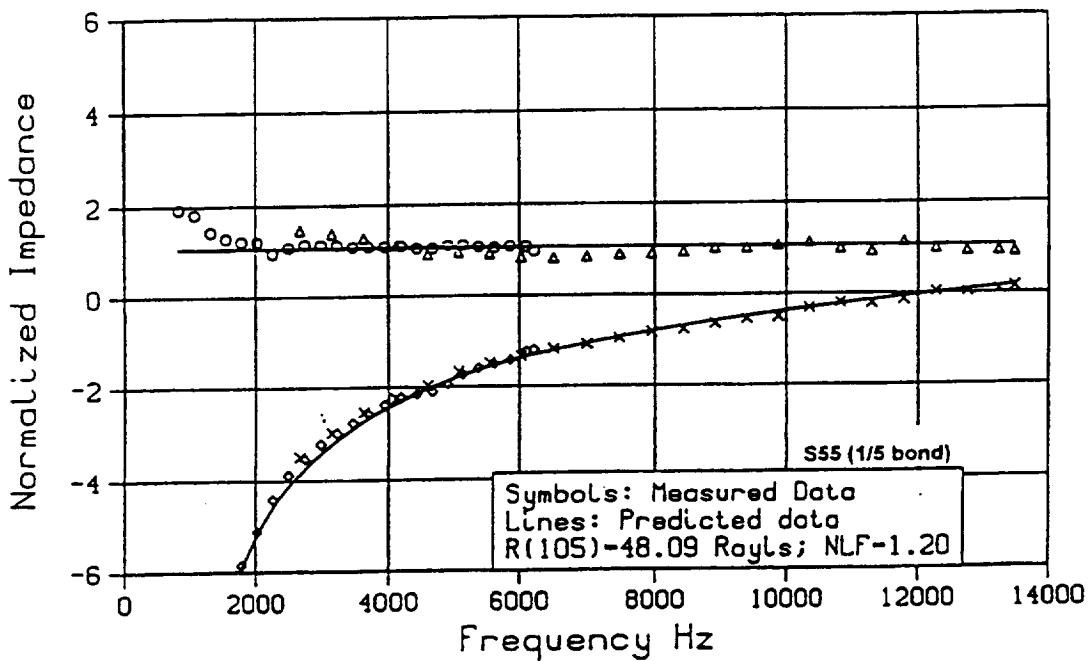


Figure 4-22

Scaling Acoustic Liner Impedance Data
1/1 Scale DDOF Linear Liner (0.9/1.5 in Core)

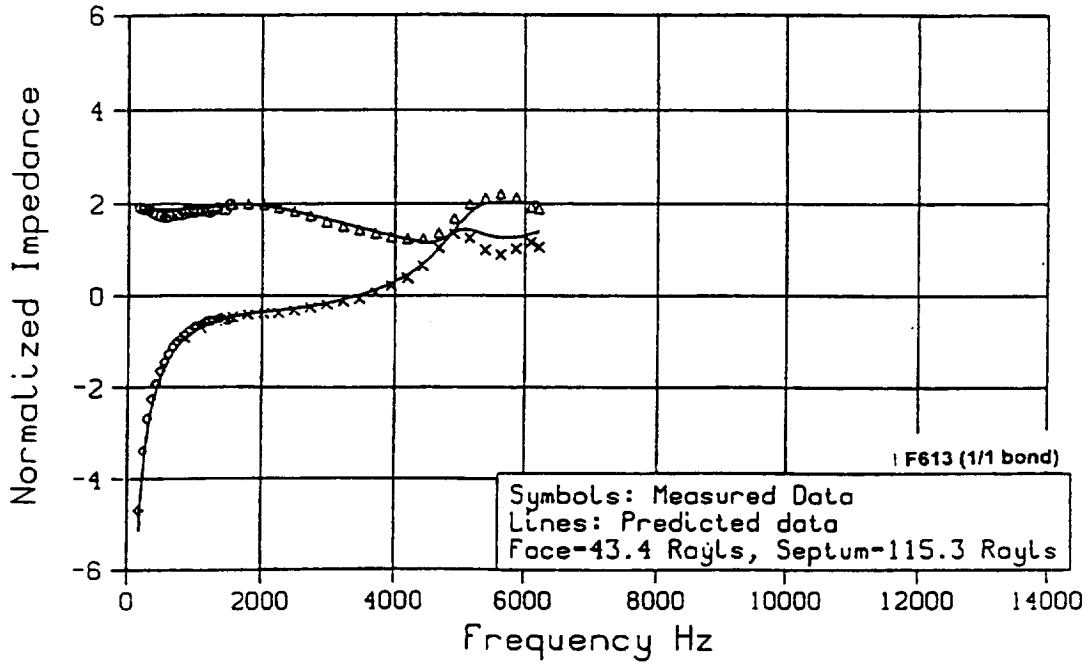
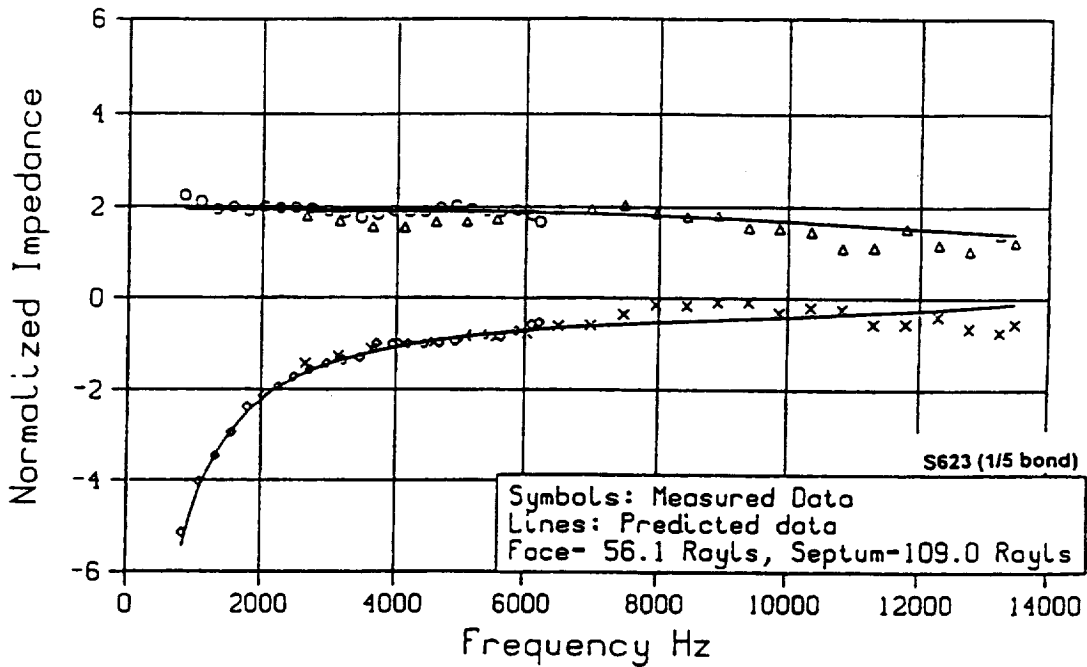


Figure 4-23

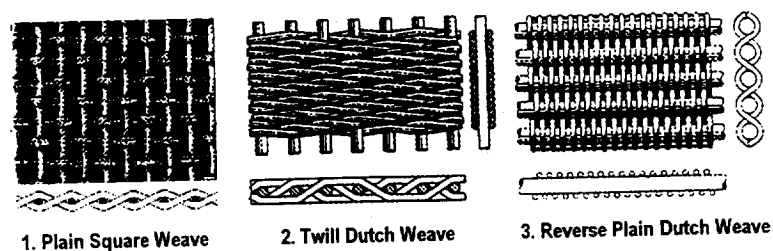
Scaling Acoustic Liner Impedance Data
1/5 Scale DDOF Linear Liner (0.18/0.3 in Core)



Several key findings, specific to linear liners are:

1. For full-scale specimens, the wire mesh is bonded to a large POA perforated plate, but for the 1/5th-scale specimens, the wire mesh is directly bonded to the core blanket. In the bonding process, the addition of the perforate plate (bonded to wire mesh) creates more blockage than the wire mesh directly bonded to the core. Wire mesh that possess a low DC flow resistance were used for full-scale specimens, whereas mesh possessing a higher DC flow resistance were used for the 1/5th-scale specimens. This causes the non-linear factor, NLF, for the full-scale liner to be higher than that for the 1/5th-scale liners. All details are shown in Table 4-4.
2. For linear liners, the sound pressure level does not play as significant a role as for perforated liners, because of the lower NLF values. Both SDOF and DDOF liner specimens show that the impedance curves overlap in the transition area (824 Hz to 1524 Hz for full-scale specimens, and 2627 to 6224 Hz for 1/5th-scale specimens) between two data sets. The acoustic resistance is close to the DC flow resistance. The resistance contribution obtained from the frequency dependent term is very small, even in the high frequency range.
3. For the 1/5th-scale wire mesh liners, the mass reactance per wave number is a real constant (the same value in all three frequency categories). In addition, its negative non-linear slope is too small to detect. For the full-scale liner, the small change in the mass reactance constant for each frequency category is caused by the perforate sheet. The slightly negative non-linear slope is also the result of the perforate plate.
4. An empirical analytical prediction model is used instead of Rice's model presented in Volume 2, Section 4.4.1. Rice's analytical prediction model provides a good understanding of linear wire mesh liner behavior. However, the plain square weave fabric style used for model development is not a popular weave style (such as the reverse plain dutch weave) to represent a mesh type linear liner acoustic treatment application. Figure 4-24 shows several different wire mesh weave styles.

Figure 4-24 Wire Mesh Weave Styles



The plain square weave is the simplest weave style (equivalent size wires are crossed over each other). Normally it has relatively weak structural strength and a higher non-linear factor ($1.2 < \text{NLF} < 1.5$) compared to other weave styles. Rohr uses this weave style for

low resistance liner applications (1 to 5 rayls @ 105 cm/sec for the mesh only and 5 to 15 rayls for bonded liners). For the reverse plain dutch weave style, the wrap wires have a smaller diameter than the shute wires and touch each other, while the heavier shute wires are woven as tightly together as possible. This weave style provides for a wide DC flow resistance range (15 to 60 rayls @ 105 cm/sec for the meshes and 30 to 120 rayls for bonded liners) and a low non-linear factor ($NLF < 1.2$). This weave style is the most popular for use in linear liner applications. The twill dutch weave style has limited application. It is normally used for very high resistance liner applications. However, it can also be used to accommodate applications that require acoustic performance characteristics that fall between the square plain weave and reverse plain dutch weave. Both reverse plain dutch weave and twill dutch weave wire meshes have very complex geometrical structure and it is extremely difficult to estimate the POA and hole diameter values by the simple method used for plain square weave wire meshes (see Volume 2, Section 4.4.1). In addition, it is not practical to use the small wire diameter and odd shape open area as design and QA criteria. It is much easier to directly use DC flow resistance ($R(105)$ and NLF) as criteria to order and inspect the wire mesh material. Rohr's data base indicates that the frequency dependent acoustic resistance is insignificant for mesh type linear liners. The liner DC flow resistance and acoustic resistance are almost the same. In this case, more accurate impedance prediction results will be produced using DC flow resistance data as input.

5. Good agreement exists between acoustic resistance predictions and data measurements for both SDOF full-scale and 1/5th-scale liner specimens. However, unusually high resistance data are found in both low and high frequency ranges for the full-scale SDOF liner specimens (F43 and F53). The problem associated with the low frequency end has been explained in the perforate liner study (Section 4.3.2). The problem associated with the high frequency end is not clear, but it is probably attributable to measurement difficulties caused by the high absolute impedance values. For the perforate samples, the acoustic resistance value is low and the absolute impedance value at the high frequency end is less than the linear liner, so the phenomenon is not as obvious for the linear liner data. However, by carefully examining the full-scale perforated liner data (e.g., F113, F22, and F32,) it actually shows a similar trend as for full-scale linear liners. One quick way to deal with this issue is to adjust the core depth such that it minimizes the reactance value and reduces the absolute impedance value.
6. Wire mesh mass reactance is determined empirically based on the DC flow resistance intercept and bonding blockage factor. The mass reactance constants for all the linear liner specimens are listed in Table 4-5. Both full-scale and 1/5th-scale SDOF liner specimens show good agreement between reactance predictions and test data. For full-scale liner specimens, the reactance data in the high frequency end is slightly skewed. This probably is caused by the same reason as mentioned in Item 5.
7. For full-scale DDOF liner specimens (F613) the predicted and measured data match well until the septum reactance term approaches the singularity point (about 4500 Hz). For the 1/5th-scale DDOF liner specimen (F623), no singularity was evidenced. The predicted

data matches the measured data obtained from the 3 cm impedance measuring system. Both resistance and reactance data measured from the 1.5 cm impedance measuring system show a small sinusoidal behavior. For DDOF liner impedance measurements, the septum core blankets on both sides have been trimmed to allow the specimens to fit into the measuring device. During the measurement, if the equipment setup can not firmly support the septum wire mesh, it can create a membranous effect and result in sinusoidal behavior. Nevertheless, the general trend still indicates that predictions and test data correlate well.

As discussed in Volume 2, Section 4.4.1, the mesh style linear liners are insensitive to grazing flow effects. Therefore, one can use the following procedure to predict acoustic impedance accurately for both full-and sub-scale linear acoustic liners. The first step is to select a semi-empirical analytical model as a prediction tool; the second step is use of DC flow resistance data as an input parameter; the third step is to estimate the mesh mass reactance based on DC flow data and bonding blockage factor; and the final step is to add the perforated plate impedance components into the analytical model (if applicable).

However, some obstacles still remain before sub-scale liners can be used to simulate full-scale acoustic treatment. The most obvious problem is that the resistance non-linear factor (or non-linear slope) and mass reactance are not scaleable. In this case, the sub-scale liner impedance data can not accurately represent the full-scale liner impedance characteristics, making the scale analysis more complex. To overcome the problem, one can slightly adjust sub-scale liner input parameters to compensate for the effects of these non-scaleable factors.

For example, Figure 4-25 shows the impedance prediction results for both full-scale and 1/5th-scale DDOF liners using the configuration defined in Table 4-4. For comparison purposes, the sub-scale impedance curve has been scaled back to the full-scale frequency range. The data indicate that at a frequency over 3000 Hz, the reactance curve of the 1/5th-scale sample deviates from the full-scale value. For data taken over 5000 Hz, the sub-scale and full-scale data do not match well; however, they fall within a small bandwidth. By adjusting the 1/5th-scale first layer core depth from 0.18 inch to 0.16 inch and septum core depth from 0.3 inch to 0.28 inch, the impedance data of the 1/5th-scale liner matches much closer to the full-scale liner. Figure 4-26 shows that the sub-scale and full-scale impedance curves match well until 5000 Hz. This 2000 Hz bandwidth improvement makes the sub-scale liner more representative of the full-scale condition.

Figure 4-25

Scaling Acoustic Liner Impedance Data
1/1 and 1/5 DDOF Acoustic Liner

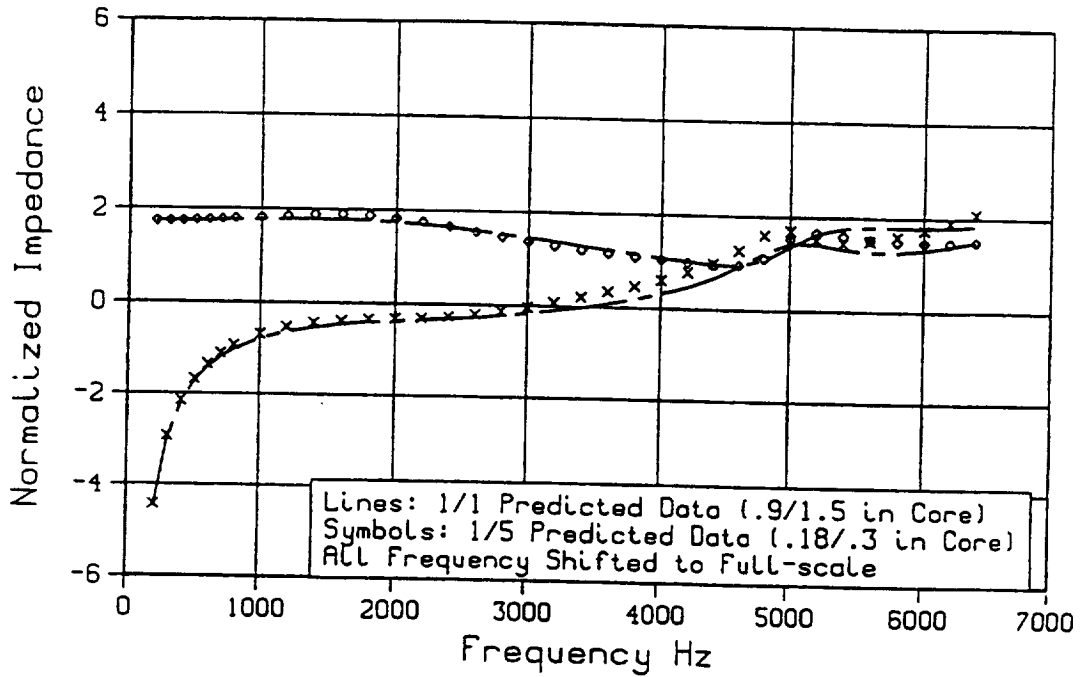
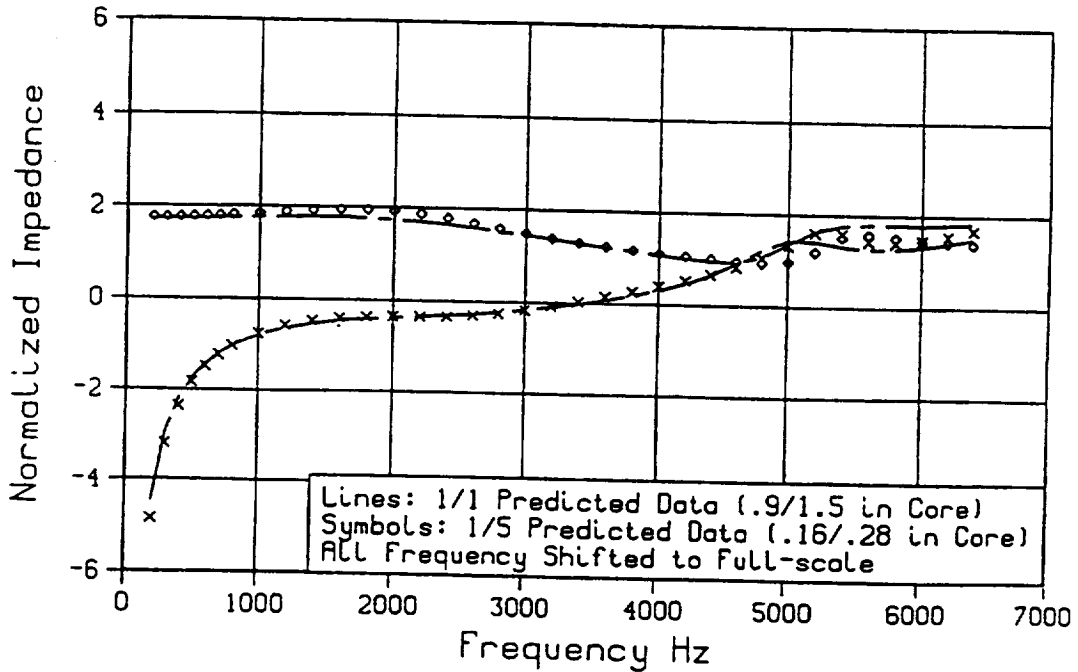


Figure 4-26

Scaling Acoustic Liner Impedance Data
1/1 and Modified 1/5 DDOF Acoustic Liner



5. Conclusions and Recommendations

Six sets of acoustic test samples with fifteen liner configurations, and three scale factors have been fabricated and tested by Rohr and GEAE. The DC flow resistance measurements and normal incidence impedance tests performed by Rohr have provided useful data to support scale treatment impedance analytical model development and validation. Rohr's analyses demonstrate that the theoretical impedance models discussed in Volume 2 can be upgraded and modified to fit both full-scale and sub-scale liners requirements. The success of the modifications is based on several key techniques and assumptions discussed in Section 4 and summarized below.

1. An exact solution is used to solve Crandall's Equation.
2. The perforate plate thickness to hole diameter ratio must be less than one for both full- and sub-scale liners to maintain a predictable discharge coefficient.
3. Effective POA and effective hole diameter values obtained from DC flow resistance data are used as input parameters for impedance calculations.
4. Non-linear behavior is applied to both resistance and reactance data. The non-linear slope constants are determined empirically.
5. DC flow resistance data is used as an input parameter to calculate linear liner impedance.
6. Wire mesh mass reactance is determined empirically based on DC flow resistance and bonding blockage.
7. Small adjustments to the core depth and wire mesh resistance can be used to compensate for non-scaleable parameters to achieve scaling treatment impedance requirements.

Excellent agreement between impedance predictions and test data provides confidence that an empirical approach can be used to modify existing impedance models to adequately handle the scaling of acoustic treatment. Although the data comparison only goes to 14000 Hz, the prediction model has the potential to extrapolate to very high frequency ranges (20000 to 30000 Hz). However, measurement of liner impedance above 14000 Hz to validate the analytical models become a major challenge for the further evaluation. In addition, other critical issues remain to be solved, such as the incorporation of grazing flow effects, especially for perforate liners; bonding problems for sub-scale liners, and noise source/acoustic modes simulation between full-scale and sub-scale liners. For these reasons, Phase II studies should concentrate on these challenging issues.

6. Appendix A - Acoustic Test Specimen Matrices

Each attached sheet in Appendix A contains a complete description of one type of test specimen. The test articles are grouped by treatment panel design and by scale. Test specimens include standard flow duct test panels mounted in frames, special instrumented duct test panels mounted in frames, and normal incidence impedance tube samples. The instrumented duct test panels include installation of features that allow two-microphone impedance measurement instrumentation to be mounted in individual honeycomb cells and a cut-out and sealed section to adapt to the DC flow resistance with grazing flow measurement apparatus.

TABLE 1-1
Acoustic Treatment Design Scaling Methods
Group 1-1 -- Full Scale Test Panel

SDOF PERFORATE LINER	GE flow duct	GE DC flow & impedance with grazing flow	Rohr impedance tubes (3&10cm)
SIZE (inch xinch)	5x12	5x12	5x12
BONDING METHOD	Perf. reticulation	Perf. reticulation	Perf. reticulation
FACE SHEET	Al perforate	Al perforate	Al perforate
Open area (POA)	10 +/- 1 (installed)	10 +/- 1 (installed)	10 +/- 1 (installed)
Hole spacing (inch)	.114 (stagger)	.114 (stagger)	.114 (stagger)
Hole diameter (inch)	.039	.039	.039
Plate thickness (in.)	.025	.025	.025
CORE	Aluminum	Aluminum	Aluminum
Core Depth (inch)	1.0	1.0	1.0
Core size (inch)	3/8	3/8	3/8
Wall thickness (in.)	.005	.005	.005
BACKPLATE	Aluminum	Plexiglas	Aluminum
Plate thickness (in.)	.032-.05	.5	.032-.05
FRAME (7.5"x14")	Yes	Yes	No
Instrumented treated panel	No	Yes	No

NOTE: See Figures 2.2-1 and 2.2-2 for frame and instrumented treated panel design

TABLE 1-2 (Revised)
Acoustic Treatment Design Scaling Methods
Group 1-2 -- 1/2 Scale Test Panel

SDOF PERFORATE LINER	GE flow duct, DC flow resistance & acoustic impedance measurement with grazing flow	Rohr impedance tubes(1.5&3cm)	GE high temperature flow resistance
SIZE (inch xinch)	5x12	5x6	5x6
BOND METHOD	Core reticulation	Core reticulation	No
FACE SHEET	Ti microporous	Ti microporous	Ti microporous
Open area (POA)	10 +/-1 (Effective)	10 +/- 1 (Effective)	10.4 +/- 1 (Exit)
Hole spacing (inch)	.055 (straight)	.055 (straight)	.055 (straight)
Hole diameter (inch)	.020	.020	.020
Plate thickness (in.)	.012	.012	.012
CORE	Aluminum	Aluminum	No
Core Depth (inch)	.5	.5	No
Core size (inch)	3/8	3/8	No
Wall thickness (in.)	.0035	.0035	No
BACKPLATE	Plexiglas	No	No
Plate thickness (in.)	.5	---	---
FRAME (7.5"x14")	Yes	No	No
Instrumented treatment panel	Yes	No	No

Effective POA considers both entry and exit sides holes.
The instrumented panel will be converted from the flow duct test panel

TABLE 1-3 (Revised)
Acoustic Treatment Design Scaling Methods

Group 1-3-- 1/5 Scale Test Panel

SDOF PERFORATE LINER	GE flow duct, DC flow resistance & acoustic impedance measurement with grazing flow	Rohr impedance tubes (1.5 & 3 cm)	GE high temperature flow resistance
SIZE (inch xinch)	5x12	5x6	5x6
BOND METHOD	Core reticulate	Core reticulate	No
FACE SHEET	Ti microporous	Ti microporous	Ti microporous
Open area (POA)	10 +/- 1 (Effective)	10 +/- 1 (Effective)	10.4 +/- 1 (Exit)
Hole spacing (inch)	.022 (straight)	.022 (straight)	.022 (straight)
Hole diameter (inch)	.008	.008	.008
Plate thickness (in.)	.005	.005	.005
CORE	Aluminum	Aluminum	No
Core Depth (inch)	.5	2-.5	No
Core size (inch)	3/8	3/8	No
Wall thickness (in.)	.0035	.0035	No
BACKPLATE	Plexiglas	No	No
Plate thickness (in.)	.5	--	--
FRAME (7.5"x14")	Yes	No	No
Instrumented treatment panel	Yes	No	No

Effective POA considers both entry and exit sides holes.
 The instrumented panel will be converted from the flow duct test panel

TABLE 2 (Revised)

Acoustic Treatment Design Scaling Methods

Group 2 -- Full-& Sub-scale Test Panels

SDOF PERFORATE LINER	GE flow duct (Full Scale)	Rohr (3&10cm) impedance tubes (Full Scale)	GE flow duct (1/2 Scale)	Rohr (1.5&3cm) impedance tubes (1/2 Scale)	GE flow duct (1/5 Scale)	Rohr (1.5&3cm) impedance tubes (1/5 Scale)
SIZE (inch xinch)	5x12	5x12	5x12	5x6	5x12	5x6
BONDING METHOD	Perf. Reticulate					
FACE SHEET	Core reticulate					
Open area (POA)	Ti microporous					
Hole spacing (inch)	12 +/-1 (installed)					
Hole diameter (inch)	12.7 +/- .5 (initial)					
Hole thickness (in.)	.117/.138 (straight)					
Plate thickness (in.)	.051					
CORE	.032					
Core Depth (inch)	Aluminum					
Core size (inch)	1.0					
Wall thickness (in.)	3/8					
BACKPLATE	.003-.005					
Plate thickness (in.)	Aluminum					
FRAME (7.5"x14")	Aluminum					
	.032-.05					
	Yes	No	Yes	No	Yes	No

Rohr's impedance measurements will include microporous face skins (no core bonded)

TABLE 3 (Revised)
Acoustic Treatment Design Scaling Methods
Group 3 -- Full-& Sub-scale Test Panels

SDOF PERFORATE LINER	GE flow duct (Full Scale)	Rohr (3&10cm) impedance tubes (Full Scale)	GE flow duct (1/2 Scale)	Rohr (1.5&3cm) impedance tubes (1/2 Scale)	GE flow duct (1/5 Scale)	Rohr (1.5&3cm) impedance tubes (1/5 Scale)
SIZE (inch x inch)	5x12	5x12	5x12	5x6	5x12	5x6
BONDING METHOD	Perf. reticulate					
FACE SHEET	Ti microporous					
Open area (POA)	8 +/-1 (installed) 9.3 +/- .5 (initial)					
Hole spacing (inch)	.122 (stagger)					
Hole diameter (inch)	.039					
Plate thickness (in.)	.025					
CORE	Aluminum					
Core Depth (inch)	1.0					
Core size (inch)	3/8					
Wall thickness (in.)	.005					
BACKPLATE	Aluminum					
Plate thickness (in.)	.032-.05					
FRAME (7.5"x14")	Yes	No	Yes	No	Yes	No

Rohr's impedance measurements will include microporous face skins (no core bonded)

TABLE 4
Acoustic Treatment Design Scaling Methods
Group 4 --Full- & Sub-scale Test Panels

SDOF	GE flow duct (Full Scale)	GE impedance test with flow (Full Scale)	Rohr (3&10cm) impedance tubes (Full Scale)	GE flow duct (1/5 Scale)	Rohr (1.5&3cm) impedance tubes (1/5 Scale)
LINEAR LINER					
SIZE (inch x inch)	5x12	5x12	5x12	5x12	5x8
BONDING METHOD	Perforate reticulation				
FACE SHEET	Stainless steel wire mesh bonded to perforate plate (RMS070 3.4-3.7 g/sq. ft.)				
Resistance (R3-ray)	90 (80-100)	90 (80-100)	90 (80-100)	90 (80-100)	90 (80-100)
Wire mesh (ray)	32	32	32	57	57
Open area (POA)	34 (initial)	34 (initial)	34 (initial)	--	--
Hole spacing (inch)	0.82 (stagger)	0.82 (stagger)	0.82 (stagger)	--	--
Hole diameter (inch)	.05	.05	.05	--	--
Plate thickness (in.)	.025	.025	.025	--	--
CORE	Aluminum	Aluminum	Aluminum	Aluminum	Aluminum
Core Depth (inch)	1.0	1.0	1.0	.2	.2
Core size (inch)	3/8	3/8	3/8	1/4	1/4
Wall thickness (in.)	.005	.005	.005	.003	.003
BACKPLATE	Aluminum	Plexiglas	Aluminum	Aluminum	Aluminum
Plate thickness (in.)	.032-.05	.5	.032-.05	.032-.05	.032-.05
FRAME (7.5"x14")	Yes	Yes**	No	Yes	No

** Instrumented cavity is required for impedance measurement

TABLE 5
Acoustic Treatment Design Scaling Methods
Group 5 --Full-& Sub-scale Test Panels

SDOF	GE flow duct (Full Scale)	Rohr flow duct (Full Scale)	Rohr (3&10cm) impeded. tube (Full-Scale)	GE flow duct (1/5 Scale)	Rohr flow duct & (1.5&3cm) impeded. tubes (1/5 Scale)
LINEAR LINER					
SIZE (inch x inch)	5x12	5.5x24	5x12	5x12	12x24
BONDING METHOD	Perforate reticulation		Core reticulation		
FACE SHEET	Stainless steel wire mesh bonded to perforate plate				
Resistance (R3-ray)	60 (45-70)	60 (45-70)	60 (45-70)	60 (45-70)	60 (45-70)
Wire Mesh (Ray)	21	21	21	37	37
Open area (POA)	34 (initial)	34 (initial)	34 (initial)	--	--
Hole spacing (inch)	0.82 (stagger)	0.82 (stagger)	0.82 (stagger)	--	--
Hole diameter (inch)	.05	.05	.05	--	--
Plate thickness (in.)	.025	.025	.025	--	--
CORE	Aluminum	Aluminum	Aluminum	Aluminum	Aluminum
Core Depth (inch)	1.0	1.0	1.0	.2	.2
Core size (inch)	3/8	3/8	3/8	1/4	1/4
Wall thickness (in.)	.005	.005	.005	.003	.003
BACKPLATE	Plexiglas	Plexiglas	Aluminum	Aluminum	Aluminum
Plate thickness (in.)	.5	.5	.032-.05	.032-.05	.032-.05
FRAME (7.5"x14")	Yes	No	No	Yes	No

TABLE 6-1
Acoustic Treatment Design Scaling Methods
Group 6-1 --Full Scale Test Panels

DOUBLE DEGREE OF FREEDOM (DDOF) LINEAR LINER		
SIZE (inch x inch)	a. GE flow duct 5x12; b. Rohr flow duct 5.5x24; c. Rohr impedance tube 5x12	
FRAME (7.5"x14")	Used for GE flow duct panel only (Item a)	
FACE SHEET BONDING METHOD	Perforate reticulation	SEPTUM BONDING METHOD
FACE SHEET	Stainless steel wire mesh bonded to perforate plate	SEPTUM SKIN
Resistance (R3)	40 (30-50)	Resistance (R4C)
Wire mesh (rayl)	15	Wire mesh (rayl)
Open area (POA)	34 (initial)	Open area (POA)
Hole spacing (inch)	0.82 (stagger)	Hole spacing (inch)
Hole diameter (inch)	.05	Hole diameter (inch)
Plate thickness (in.)	.025	Plate thickness (in.)
FACE CORE	Aluminum	SEPTUM CORE
Core Depth (inch)	.90	Core Depth (inch)
Core size (inch)	3/8	Core size (inch)
Wall thickness (in.)	.003 or .005	Wall thickness (in.)
R3 PANEL**	Required prior to 2DOF bonding	BACKPLATE
Size (inch x inch)	6x6 to 12x12	Plate thickness (in.)
		Core reticulation on wire mesh side; Perf. reticulation on perforate plate side
		Stainless steel wire mesh bonded to perforate plate
		100 (85-115)
		27
		34 (initial)
		0.82 (stagger)
		.05
		.025
		Aluminum
		1.50
		3/8
		.003 or .005
		Aluminum
		.032-.05

** Additional panel used for R3 inspection prior to bonding

TABLE 6-2
Acoustic Treatment Design Scaling Methods
Group 6-2 --1/5 Scale Test Panels

DOUBLE DEGREE OF FREEDOM (DDOF) LINEAR LINER			
a. GE flow duct 5x12; b. Rohr flow duct 5.5x24; c. Rohr impedance tube 5x8			
Used for GE flow duct panel only (item a)			
SIZE (inch x inch)	PERFORATE RETICULATION	SEPTUM BONDING METHOD	CORE RETICULATION ON BOTH SIDES
FRAME (7.5"x14")			
FACE SHEET BONDING METHOD	Perforate reticulation	SEPTUM SKIN	Core reticulation on both sides
FACE SHEET	Stainless steel wire mesh only	Resistance (R4C)	Stainless steel wire mesh only
Resistance (R3-rayls)	40 (30-50)	Wire class	90 (75-105)
Wire class	C13 (27 rayls)	SEPTUM CORE	C4 (42 rayls)
FACE CORE	Aluminum	Core Depth (inch)	Aluminum
Core Depth (inch)	.18	Core size (inch)	.3
Core size (inch)	1/4	Wall thickness (in.)	1/4
Wall thickness (in.)	.003	BACKPLATE	.003
R3 PANEL**	Required prior to 2DOF bonding		Aluminum
Size (inch x inch)	6x6 to 12x12	Plate thickness (in.)	.032-.05

** Additional panel used for R3 inspection prior to bonding

TABLE 7-1
Acoustic Treatment Design Scaling Methods
Group 7-1 -- Full- & Sub-scale Test Panel

RIGID FOAM BULK LINER	GE flow duct (Full Scale)	GE flow duct (1/2 Scale)	GE flow duct (1/5 Scale)
SIZE (inch x inch)	5x12	5x12	5x12
BONDING METHOD	Perf. reticulation	Perf. reticulation	Perf. reticulation
FACE SHEET	Al perforate	Al perforate	Al perforate
Open area (POA)	34 (initial)	34 (initial)	34 (initial)
Hole spacing (inch)	0.82 (stagger)	0.82 (stagger)	0.82 (stagger)
Hole diameter (inch)	.05	.05	.05
Plate thickness (in.)	.02 to .025	.02 to .025	.02 to .025
CORE	Aluminum	Aluminum	Aluminum
Core Depth (inch)	1.0	.5	.21
Core size (inch)	3/8	3/8	3/8
Wall thickness (in.)	.003 to .005	.003 to .005	.003 to .005
BULK MATERIAL	Ultramet 300 ppi	Ultramet 400 ppi	Ultramet 600 ppi
Thickness (inch)	1.0	.5	.21
flow Resistance	100 rays/cm	200 rays/cm	500 rays/cm
BACKPLATE	Aluminum	Aluminum	Aluminum
Plate thickness (in.)	.032-.05	.032-.05	.032-.05
FRAME (7.5"x14")	Yes	Yes	Yes

TABLE 7-2
Acoustic Treatment Design Scaling Methods
Group 7-2 -- Full- & Sub-scale Test Panel

RIGID FOAM BULK LINER	Flow resistance and normal impedance measurements	
SCALING FACTOR	Full	1/2
SIZE (inch x inch)	5x8	5x8
BULK MATERIAL **	Ultramet 300 ppi	Ultramet 400 ppi
Thickness (inch)	1.0	.5
Approximate DC flow Resistance	100 rays/cm	200 rays/cm
ROHR RAYLOMETER	3 cm tube	3 cm tube
ROHR IMPEDANCE TUBES	3cm & 1.5cm tubes	3cm & 1.5cm tubes
GE HIGH TEMP FLOW RESISTANCE	1.25 inch tube ++	1.25 inch tube++
		1/5
		5x8
		Ultramet 600 ppi
		.21
		500 rays/cm
		3 cm tube
		3cm & 1.5cm tubes
		1.25 inch tube++

** Additional measurement will be conducted with selected perforate face plates

++ Stainless steel sample holder sleeve is required (inner dia. = 1.25 inch; outer dia.=1.75 inch)

7. **Appendix B - Inspection Plan**

INSPECTION PLAN
Acoustic Treatment Design Scaling Methods
S.O. PL310
12-17-93

This inspection plan will delineate the inspection requirements and process controls for the acoustic scaling test panel project.

Raw Materials

Metallic materials will have heat & lot traceability. Honeycomb and wire mesh materials may be obtained from excess cut-off of production hardware. Adhesive materials and bond primers will be traceable to lot numbers and expiration dates.

Fabrication Planning

An "acoustic panel fabrication request" work sheet, will be prepared for each panel, will define the configuration and manufacturing steps used to fabricate each panel. These records will be retained by Rohr for future reference.

Dimensional inspection

Panel dimensional inspection will consist of the overall length, width, hole size, hole spacing and percentage of open area.

Acoustic Treatment Test⁷

An engineering laboratory raylometer will be use to collect air flow data and will be evaluated by engineering at each step of the bond process for acceptance of the acoustic values.

N.D.E.

Non-destructive testing will consist of a visual inspection of the panel surface for workmanship irregularities, defects and contamination. A tap test may be performed as necessary to assess voids and delaminations.



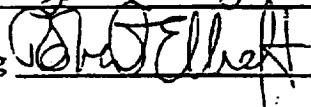
Sample Tray Holding Fixture

Panels which are mounted in a sample tray for test purposes, will be inspected for overall length per GEAE instructions.

Inspection Reports

Inspection reports submitted to GEAE will consist of a matrix identifying the panel configuration and the raylometer values.

Concurrence:

Rohr Engineering  Rohr Q.A.  12/17/93
GEAE Engineering  12/17/93

8. Appendix C - High Temperature DC Flow Resistance Tests

8.1 Steady (DC) Flow Resistance Testing

The DC flow resistance properties of porous materials are closely related to their acoustic impedance characteristics. The methods for the measurement and correlation of DC flow resistance data are described in considerable detail by Motsinger, Syed and Manley¹. The basic method for the measurement of DC flow resistance is described below.

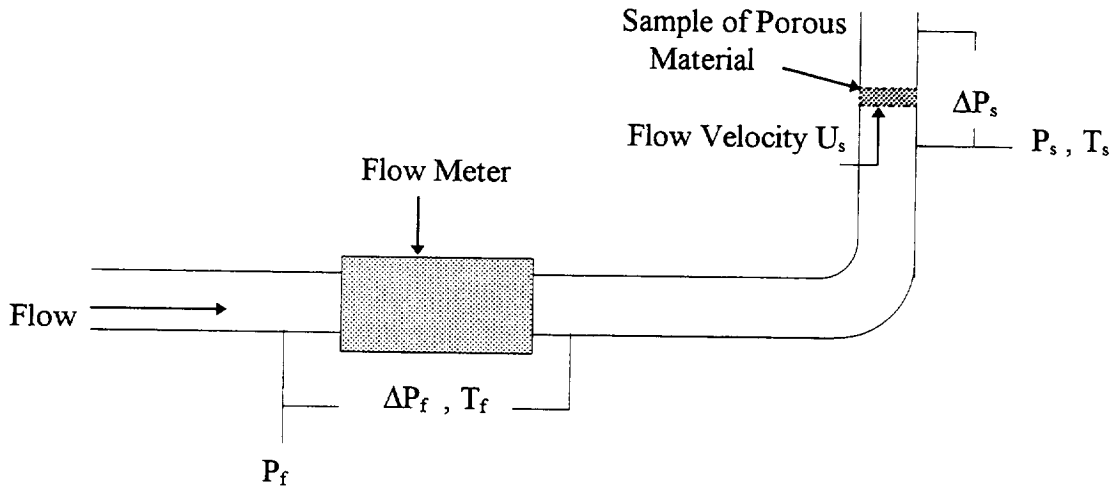


Figure C-1 Basic DC Flow Resistance Apparatus

A typical apparatus for the measurement of DC Flow Resistance of a porous sample is schematically illustrated in Figure C-1 above. It shows the parameters that have to be measured during a test. The flow may either be sucked or blown through the sample. The system shown above is of the blowing type. At a given flow condition, the flow meter measures the mass flow rate using the parameters shown. The flow velocity through the sample, U_s , is computed as follows:

$$U_s = \frac{(\text{mass flow rate})}{\rho_s A_s} \quad (\text{C-1})$$

and the DC Flow Resistance of the sample is defined as

$$R_s(U_s) = \frac{\Delta P_s}{U_s} \quad (\text{C-2})$$

¹ R. E. Motsinger, A. A. Syed and M. B. Manley, "The Measurement of the Steady Flow Resistance of Porous Materials", Paper No. AIAA-83-0779, AIAA 8th Aeroacoustic Conference, April 1983.

where

ΔP_f	is the pressure difference across the Flow Meter (psid)
P_f	is the pressure upstream of the Flow Meter (psia)
T_f	is the temperature of air upstream of the Flow Meter ($^{\circ}\text{R}$)
ΔP_s	is the pressure difference across the sample (dynes/cm ²)
U_s	is the calculated mean flow velocity just upstream of the sample
ρ_s	is the calculated fluid density just upstream of the sample (gm/cm ³)
A_s	is the area of the porous sample (cm ²) used in equation (1)
$R_s(U_s)$	is the DC flow resistance (cgs Rayl) of the porous sample .

Generally the measured DC flow resistance data are normalized to specified reference temperature and pressure values, T_0 and P_0 , just upstream of the sample. At GE Aircraft Engines, we use $T_0 = 70^{\circ}\text{F}$; $P_0 = 29.92\text{ IN. Hg}$.

8.2 High Temperature DC Flow Resistance Tests

These tests were designed to determine the scaling laws governing the temperature conditions in which a porous material has to operate. The experimental apparatus is schematically illustrated in Figure C-2 below.

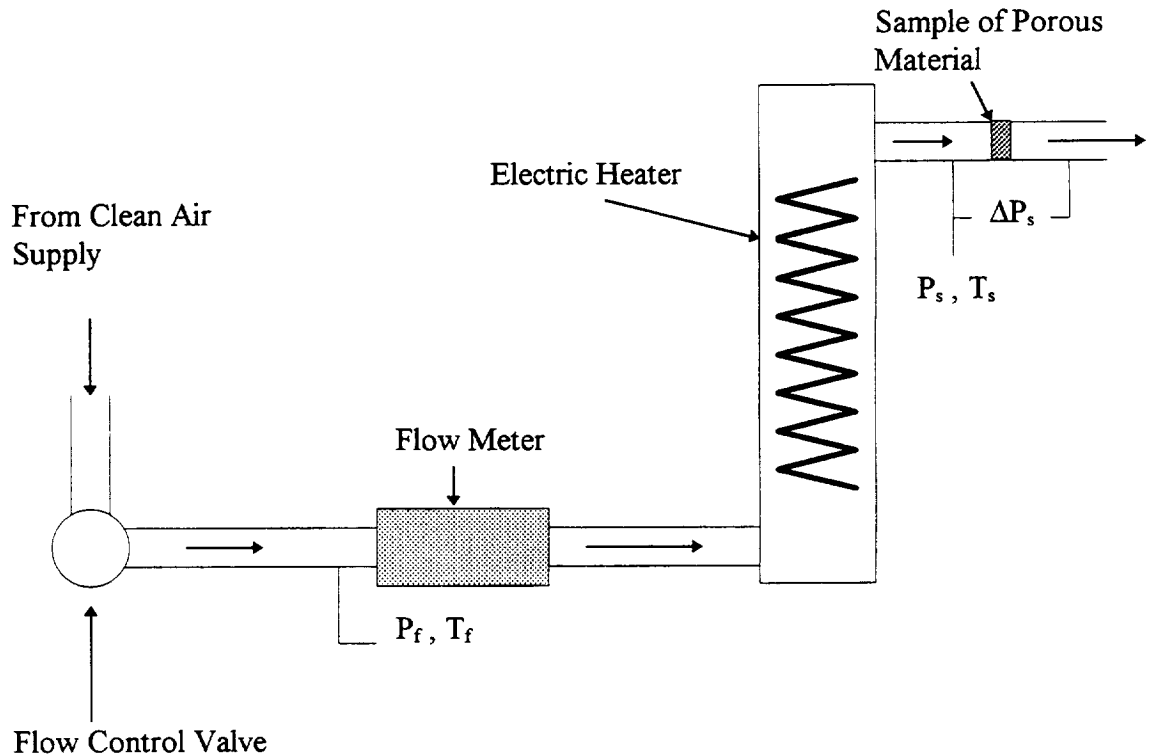


Figure (C-2) High Temperature DC Flow Resistance Apparatus

A 25 kWatt heater was used to heat the air flowing through the system. Flow-Dyne Critical Flow Nozzle flow meters were employed to measure the mass flow rate through the apparatus. Critical flow is characterized by choked flow in the nozzle throat. Under these conditions, a fixed pressure ratio exists between the inlet pressure to the nozzle and the pressure in the throat. Pressure changes downstream of the throat can not affect the upstream pressure. The mass flow rate becomes dependent upon the upstream pressure and temperature only. Thus the mass flow rate, w , is given by

$$w = \frac{KP_f}{\sqrt{T_f}} \quad (C-3)$$

where K is the calibration coefficient supplied with each nozzle.

8.3 Calibration of the Apparatus

Three types of instruments used on this series of tests required calibration:

- (1) Critical flow nozzles
- (2) Pressure Sensors
- (3) Temperature Gages

8.3.1 Critical flow nozzles

Flow-dyne Critical Flow Nozzles are converging-diverging nozzles that operate on the principle of critical flow, as described above. At pressure ratios as low as 1.2, the flow rate through the nozzle varies almost linearly with the upstream pressure and is insensitive to downstream pressure fluctuations. The manufacturer provides flow coefficient curves as a function of pressure ratio. The overall system uncertainty quoted by the manufacturer is 0.75% traceable to the National Bureau of Standards. There are no moving parts to affect reliability and therefore, no additional calibration required. The nozzles require two measurements to calculate the physical mass flow rate: inlet pressure and inlet temperature. The nozzle exit pressure is monitored to insure that the critical pressure ratio across the nozzle is 1.2 or greater.

As a further verification, the critical flow nozzles were checked against Cox Series 12 flow stand rotometers in the range of interest. These rotometers are on a regular calibration cycle in the Standards lab and are traceable to the National Bureau of Standards. Agreement was within approximately 2% of reading.

8.3.2 Pressure Sensors

Three types of pressure measuring devices were used in this program: (1) Heise digital transducers, (2) Druck Model 601 digital pressure indicator and (3) Mensor Pressure Sensor. The Heise transducers were used for the critical flow nozzle pressure measurements, the Druck

was used for direct measurement of the static pressure upstream of the test sample, and the Mensor was used for barometric pressure measurement. The Heise transducers were user checked by the Druck transfer standard to the labeled uncertainty of 1% full scale. Full scale for upstream was 200 in. Hg. and the full scale for the downstream were 100 in. Hg. Both the Druck and the Mensor were calibrated by the Evendale Standards Lab on the established cycles by a traceable standard. The uncertainty of the Druck is labeled .05% of full scale and it was used on the 5 psid scale. The labeled uncertainty of the Mensor is 0.04% full scale and its range is 40 IN., Hg. absolute.

8.3.3 Temperature Gages

Temperature measurements were made using a Fluke Model 2240C Data Logger with type K thermocouples. Calibration of the Fluke was user checked with a Model 1100 Ectron Thermocouple Simulator to within 1 degree F over the range of interest. The Ectron is calibrated in the Standards Lab to an uncertainty of approximately 0.2 degrees F.

8.4 Test Procedure

The test procedure required the setting of mass flow rates through the flow meter during a measurement. These flow rates needed to be independent of the sample being tested. In order to arrive at a sensible test procedure, the following criteria were considered.

- **Same Velocities:** this means that the flow velocity, U_s , to be used at high temperature is the same as that used at reference temperature. This condition requires that the mass flow rate $w(T_s)$, at temperature T_s , is given by

$$w(T_s) = \frac{P_s}{P_0} \frac{T_0}{T_s} w_0 \quad (C-4)$$

where w_0 is the mass flow rate at reference temperature T_0 .

- **Same Mach Numbers:** this requires that the measurements be made at the same values of flow Mach numbers at all temperatures. This condition requires that the mass flow rate $w(T_s)$, at temperature T_s , is given by

$$w(T_s) = \frac{P_s}{P_0} \left(\frac{T_0}{T_s} \right)^{0.5} w_0 \quad (C-5)$$

- **Same Reynolds Numbers:** this requires that measurements should be made at the same values of the Reynolds Number at all temperatures. This condition requires that the mass flow rate $w(T_s)$, at temperature T_s , is given by

$$w(T_s) = \left(\frac{T_0}{T_s} \right)^{0.75} w_0 \quad (C-6)$$

The variations of the ratio $w(T_s)/w_0$ against the temperature $T_s(^{\circ}R)$ for the above three criteria are plotted in Figure C-3. The "equal Mach numbers" criterion was used to set flow rates during the tests because it involved minimum variation in the mass flow rate over the temperature range $530^{\circ}R - 1600^{\circ}R$ for a specified flow velocity U_s .

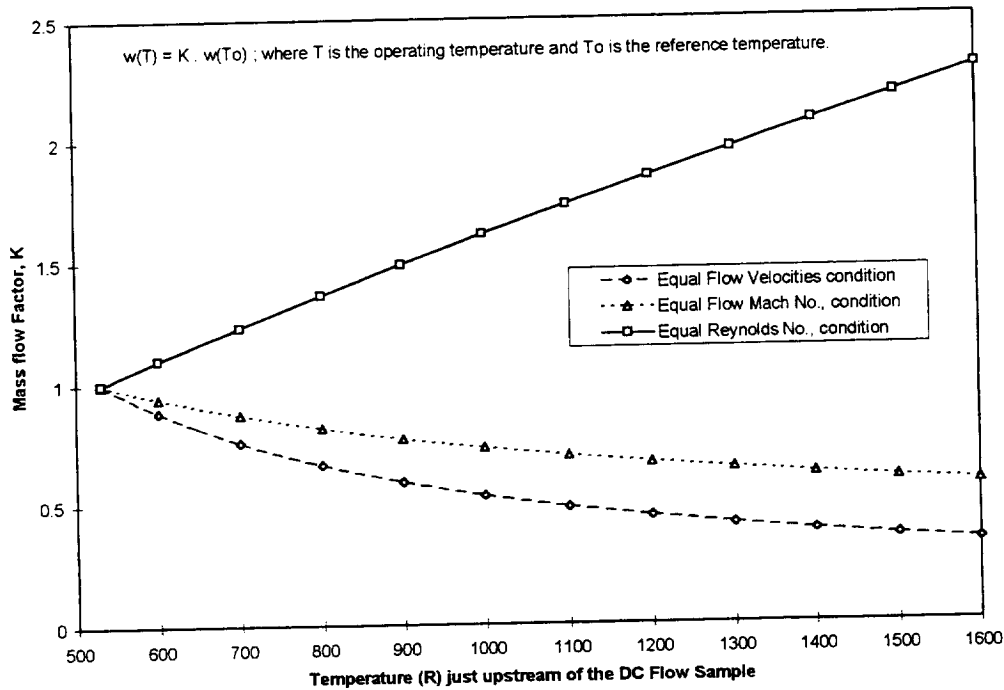


Figure (C-3) Variation of the Mass Flow Rate versus Temperature Just Upstream of the DC Flow Sample

Because of the thermal inertia of the electric heater, it was difficult to control the temperature T_s of the air flow into the sample. Moreover, due to heat transfer through the walls of the pipe upstream of the sample holder, the temperature of air flowing into the sample was not uniform. This problem was more severe at the higher flow temperatures and low flow velocities. Temperature was measured both upstream and downstream of the test sample, showing significant temperature difference between upstream and downstream locations. The average value of the two measured temperatures was used as the sample temperature T_s .

8.5 Test Results

DC flow data were measured on three samples covering a range of porous sheet materials. The first sample was a perforated sheet of 9.8% porosity. The diameter of the holes in this sheet was greater than the sheet thickness, which is representative of punched holes. The second test sample was made of a wiremesh diffusion bonded to a perforated sheet, representing linear sheet materials. The third sample was a micro-porous sheet with laser drilled holes of very small diameter (0.005 - 0.010). DC flow resistance tests were performed on test samples at ambient (room) temperature, 400°F, 700°F and 1000°F.

The measured DC flow data are tabulated in Tables C-1, C-2 and C-3. The “corrected” data are normalized to reference values of temperature and pressure (70°F and 29.92 IN. Hg.).

Nominal Temp degF	Us cm/sec	DP/Us cgs rayls	Tup deg F	Tdn deg F	Ts deg F	Correct Usc cm/sec	Correct DP/Usc cgs rayls
Room	31.38	3.95				30.65	3.94
	59.38	7.08				58.02	7.06
	88.59	10.35				86.60	10.32
	115.58	13.66				113.05	13.62
	145.55	17.67				142.51	17.62
	173.54	21.45				170.11	21.39
400 F	40.04	2.76	397	309	353	16.98	1.92
	74.53	5.18	399	309	354	31.48	3.61
	105.78	7.17	410	317	363.5	43.71	4.94
	143.03	9.69	393	307	350	61.23	6.78
	186.09	12.82	396	321	358.5	79.25	8.95
	223.93	15.24	407	332	369.5	93.35	10.54
700F	48.27	2.43	685	549	617	12.32	1.36
	85.27	4.45	703	512	607.5	21.19	2.47
	126.28	6.50	707	518	612.5	31.21	3.59
	198.78	9.75	713	548	630.5	48.74	5.37
	216.08	10.88	699	563	631	54.13	6.05
	252.88	12.51	707	609	658	62.64	6.92
1000F	95.79	4.10	949	725	837	17.01	1.97
	143.59	6.15	1005	715	860	23.83	2.87
	178.85	7.40	1000	713	856.5	29.87	3.46
	241.08	9.72	997	694	845.5	40.45	4.55
	283.92	11.41	1000	771	885.5	47.51	5.34
	332.43	13.54	995	843	919	56.03	6.35

Table C-1 High Temperature DC Flow Resistance Measured for 9.8% Porosity Perforated Steel Sheet

Nominal Temp degF	Us cm/sec	DP/Us cgs rayls	Tup deg F	Tdn deg F	Ts deg F	Correct Usc cm/sec	Correct DP/Usc cgs rayls
Room	31.41	84.94				30.57	84.47
	59.11	105.10				57.72	104.51
	87.79	122.68				86.12	121.99
	114.88	139.36				113.29	138.57
	144.34	157.83				143.29	156.94
	170.36	173.87				170.25	172.89
400 F	40.45	95.12	405	312	358.5	16.94	65.88
	73.32	113.78	395	354	374.5	31.49	79.49
	104.11	129.14	411	373	392	43.50	88.97
	141.08	140.75	390	351	370.5	61.91	98.76
	182.38	158.78	401	363	382	78.95	110.34
	217.37	173.82	408	374	391	93.57	120.07
700F	48.41	96.98	691	534	612.5	12.30	54.21
	84.49	118.74	703	608	655.5	21.20	65.86
	124.19	137.13	707	637	672	31.19	75.87
	190.38	152.83	702	633	667.5	48.74	84.82
	210.91	160.84	702	631	666.5	54.26	89.27
	244.70	172.44	699	640	669.5	63.74	95.89
1000F	96.20	125.43	995	800	897.5	16.34	58.81
	140.76	144.01	1005	867	936	23.82	67.18
	175.17	155.08	1009	886	947.5	29.70	72.19
	235.51	175.66	1018	934	976	40.05	81.40
	274.52	187.61	1013	930	971.5	47.43	87.16
	318.86	202.18	1012	947	979.5	55.83	93.97

Table C-2 High Temperature DC Flow Resistance Measured for Wire-Mesh on Perforated Steel Sheet

Nominal Temp degF	Us cm/sec	DP/Us cgs rayls	Tup deg F	Tdn deg F	Ts deg F	Correct Usc cm/sec	Correct DP/Usc cgs rayls
Room	31.06	130.74					
	58.47	211.54				30.47	130.37
	86.62	298.16				57.83	210.94
	111.76	396.51				86.82	297.32
	136.30	503.47				114.03	395.39
	159.64	606.14				142.32	502.05
						171.09	604.43
400 F	40.38	105.01	406	392	399	16.88	72.66
	72.96	160.65	393	388	390.5	31.55	112.43
	104.45	203.97	414	386	400	43.70	140.17
	140.21	266.03	390	339	364.5	62.56	186.67
	176.81	335.37	405	353	379	78.14	232.26
	207.65	408.42	407	363	385	93.61	282.36
700F	48.00	102.27	697	658	677.5	12.10	56.94
	84.20	152.32	700	721	710.5	21.29	84.65
	121.02	199.98	687	711	699	31.56	112.08
	186.21	262.15	706	652	679	48.32	145.12
	207.44	297.48	710	691	700.5	54.16	164.26
	233.43	339.38	697	628	662.5	63.18	188.97
1000F	94.92	140.93	958	958	958	16.89	67.37
	139.29	192.55	1002	1056	1029	23.82	89.96
	172.20	233.03	999	1073	1036	29.93	109.04
	230.04	297.03	1011	882	946.5	40.49	138.13
	263.61	342.90	1012	865	938.5	47.30	159.38
	300.98	403.18	1010	847	928.5	55.68	187.59

Table C-3 High Temperature DC Flow Resistance Measured for Micro-Porous Perforated Stainless Steel Sheet

The DC flow data, as measured, are plotted in Figure C-4, C-5, and C-6. Three plots are of DC flow resistance (cgs Rayls) against the mean flow velocity through the test sample at constant temperature. Notice that increasing temperature causes reduction in the slope of the DC flow plot. This means that these materials become more "linear" at high temperatures.

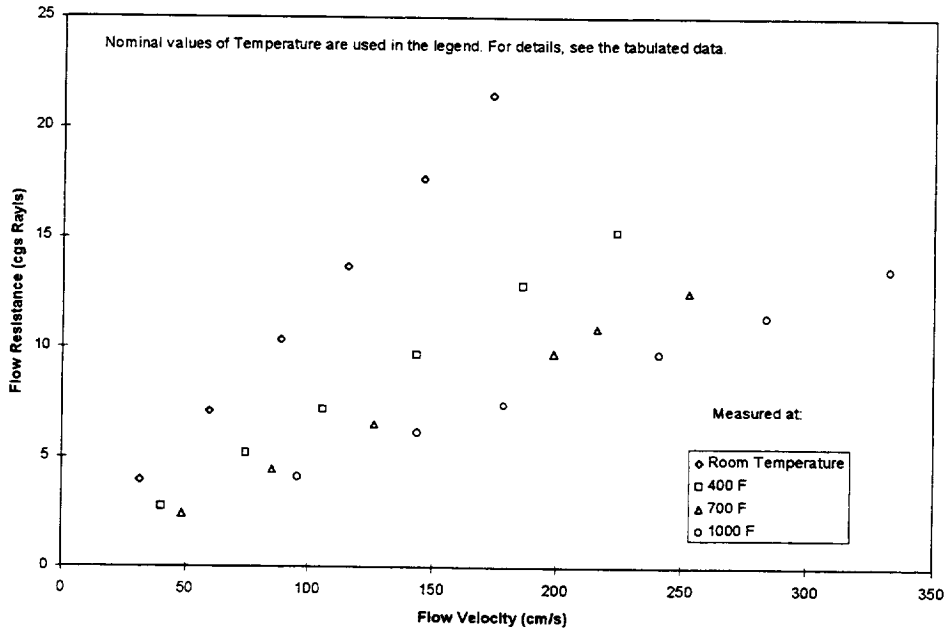


Figure (C-4) High Temperature DC Flow Resistance Measured for Perforated Steel Sheet Sample of 9.8% Porosity

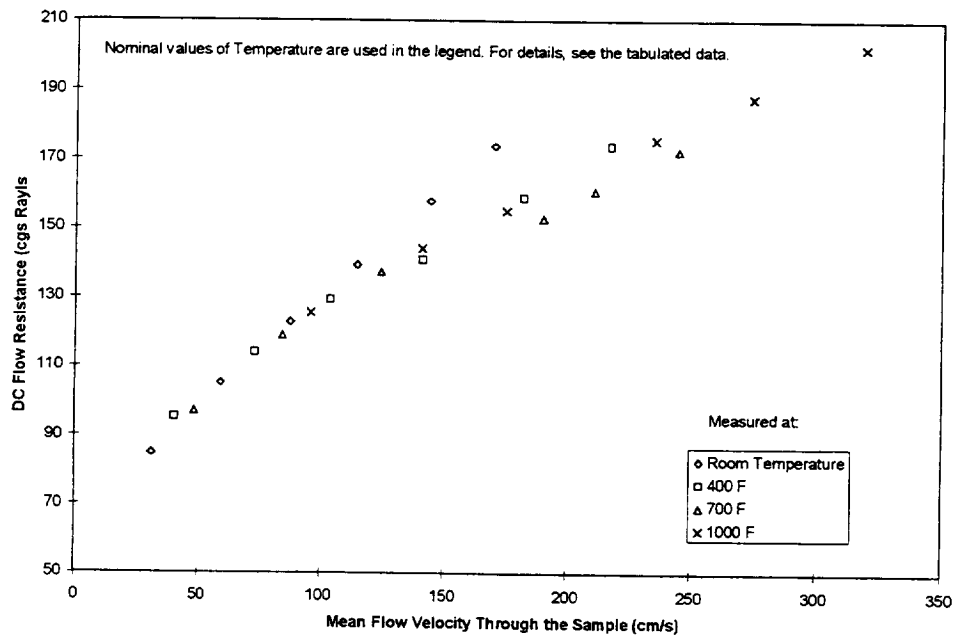


Figure (C-5) High Temperature DC Flow Resistance Measured for Wiremesh Diffusion Bonded on Perforated Sheet

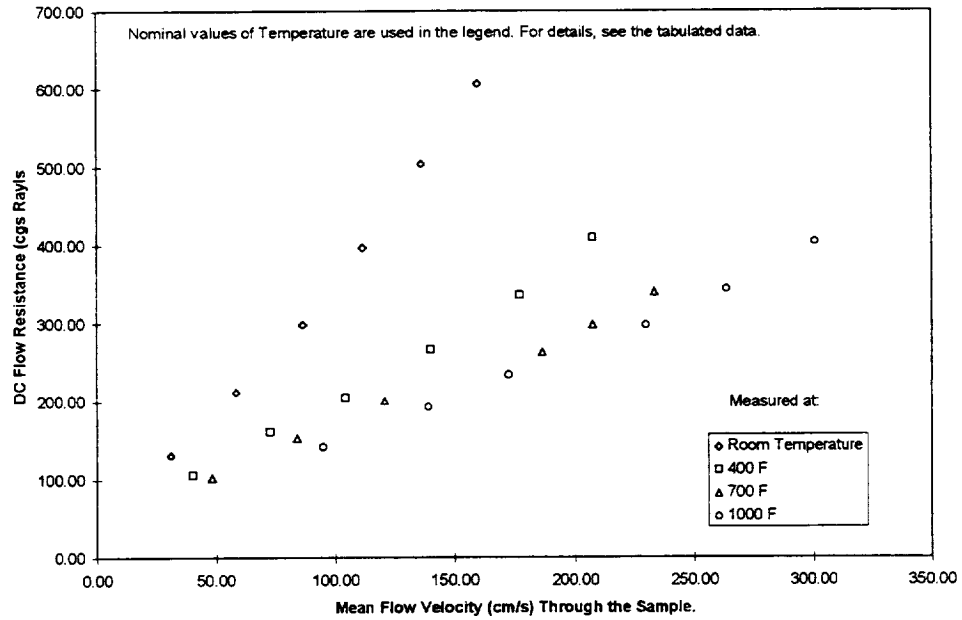


Figure (C-6) High Temperature DC Flow Resistance Measured for Stainless Steel Microporous Perforated Sheet

The data normalized to reference values of temperature and pressure are plotted in Figures C-7, C-8, and C-9. Note that the normalized high temperature DC flow resistance data collapse on the curve for the data measured at room temperature.

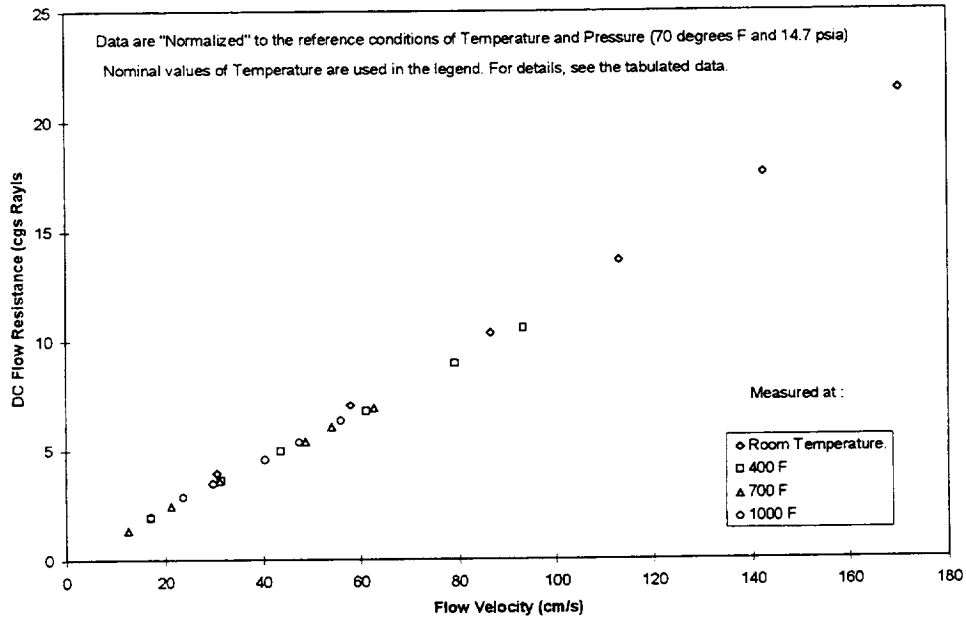


Figure (C-7) High Temperature DC Flow Resistance Measured for Perforated Steel Sheet, 9.8% Porosity Normalized to Reference Conditions

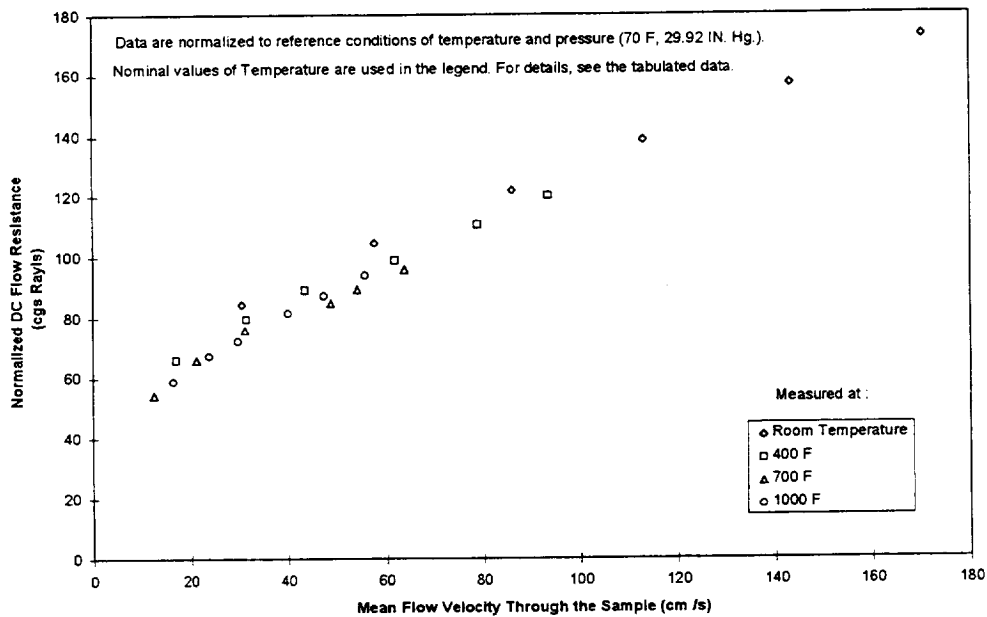


Figure (C-8) High Temperature DC Flow Resistance Measured for Wiremesh on Perforated Sheet, Normalized to Reference Conditions

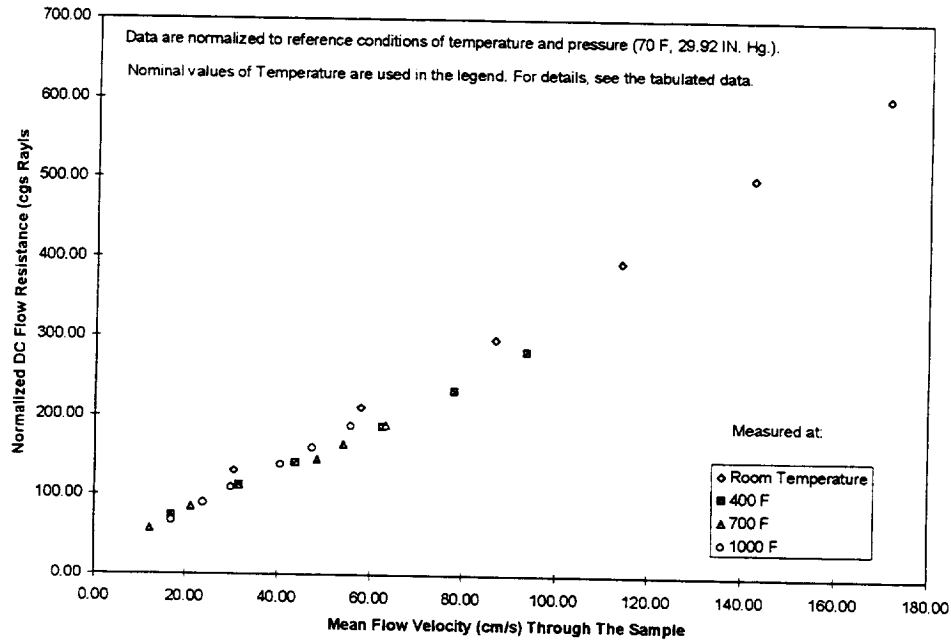


Figure (C-9) High Temperature DC Flow Resistance Measured for Microporous Perforated Sheet, Normalized to Reference Conditions

The method used to normalize these data was developed by Motsinger, Syed and Manley (see Reference 1). This method is based on the principle of dynamic similarity and hence is independent of any particular relationship between the sample resistance and the mean fluid velocity into it. It is shown in Reference 1 that

$$\left\{ \frac{\Delta P}{U} \right\}_{T_0, P_0} = \left\{ \frac{\Delta P}{U} \right\}_{T, P} \left(\frac{\mu_0}{\mu} \right) \quad (C-7)$$

$$\{U\}_{T_0, P_0} = \{U\}_{T, P} \left(\frac{\rho}{\rho_0} \right) \left(\frac{\mu_0}{\mu} \right) \quad (C-8)$$

where

- T is the temperature under test conditions just upstream of test sample
- T₀ is a reference temperature (70° F)
- P is the pressure under test conditions just upstream of test sample
- P₀ is a reference pressure (14.7 psia)
- U is the mean fluid velocity just upstream of the test sample (cm/sec)
- ρ is the density of the fluid under test conditions just upstream of test sample
- ρ₀ is the density of the fluid at reference temperature and pressure

- μ is the absolute coefficient of viscosity of the fluid at temperature T
- μ_0 is the absolute coefficient of viscosity of the fluid at temperature T_0
- ΔP is the pressure drop (dynes /sq. cm) measured across the sample corresponding to the mean fluid velocity u.

For most materials of practical interest, the D.C. Flow resistance can be described by an equation of the form

$$\frac{\Delta P}{U} = A + BU \quad (C-9)$$

where A and B are constants to be determined by a DC flow measurement.

Clearly, in addition to the geometrical parameters of the test sample (porosity, thickness, hole diameter etc.), the values of A and B also depend on the values of temperature T, pressure P, density ρ and viscosity μ of the fluid just upstream of the sample. The above scaling laws suggest that values A_0 and B_0 measured at "room temperature and pressure" (T_0, P_0) can be used to determine the values A and B at any other temperature and pressure (T,P) as follows:

$$A(T, P, \mu) = A_0(T_0, P_0, \mu_0) \frac{\mu}{\mu_0} \quad (C-10)$$

$$B(T, P, \mu) = B_0(T_0, P_0, \mu_0) \frac{\rho}{\rho_0} = B_0(T_0, P_0, \mu_0) \frac{P}{P_0} \frac{T_0}{T} \quad (C-11)$$

The simple relationship of Equation C-9 may not perfectly model the D. C. Flow resistance of all materials. However, we can still measure the D. C Flow data at "room temperature and pressure" and use the scaling laws of Equations C-7 and C-8 to calculate the DC flow resistance characteristics at any other temperature and pressure.

9. Appendix D - Technical Issues for Fabrication of Treatment Samples

9.1 Micro-perforated Specimens

The titanium thin foil micro-perforated face sheets required laser drilling due to the small diameter hole requirement. Laser drill vendors encountered difficulty maintaining accurate hole geometry. The best drill process provided holes which were "tapered" with the laser pulse entry side of each hole being larger than the exit side. As a result, the micro-perforated foils were produced at a very high cost and required extended lead times.

Adhesive reticulation techniques for the micro-perforated acoustic panels also proved difficult. The preferred method of adhesive reticulation in acoustic sandwich bonding is "perforate" reticulation. This method enables accurate control of adhesive flow and minimizes acoustic blockage. For the Treatment Scaling program it was found that unsupported film adhesive can be reticulated for perforate hole diameters in the 0.020 inch and above range. Perforate acoustic panels with holes less than 0.020 inches in diameter must be "core" reticulated. "Core" reticulation results in higher acoustic blockage due to adhesive flow into the adjacent perforate hole.

Excessive adhesive blockage was encountered on six of the micro-perforated acoustic samples. In order to obtain optimum acoustic values these panels were lightly grit blasted to remove excess adhesive. This method would prove impractical on a production basis, although one alternative may be to use a low viscosity sprayable adhesive.

9.2 Flow Duct Frames

Wood was selected as the best material alternative for frame construction due to advantages in weight, machineability, and joining (dowels with carpenter's glue). Each of the framed acoustic samples required a "custom" made frame due to dissimilarities in face sheet, core, and back skin thickness. Frame fabrication proved costly and time consuming. Polysulfide sealant was selected for use in sealing face-sheet-to-frame edges due to its high viscosity.

9.3 Plexiglass Bonding

Several resins were screened for their ability to bond plexiglass-to-core. Considerations included bond strength, ability to cure at room temperature, and clarity. A polyester casting resin (Evirotex Lite Resin) was found to be best suited for the application. Problems were encountered when it was found that the 0.50 inch thick plexiglass material was variable in thickness and flatness. Each required machining of the periphery prior to bonding to the frame assembly.

9.4 Instrumentation

D C flow partitions were prefabricated from sheared sheet aluminum, which was assembled then brazed. In order to control the dimensional conformity accurately, a welding jig was fabricated and utilized. Installation of the partitions required that the honeycomb core be cutout, the partition inserted, then a separated piece of core placed inside the partition prior to cure. A matched set of cutting dies was required for both inner and outer core cutting. Alignment of the D C flow partition and the cutout in the plexiglass also required fixturing during bonding.

REPORT DOCUMENTATION PAGE			Form Approved OMB No. 0704-0188	
Public reporting burden for this collection of information is estimated to average 1 hour per response, including the time for reviewing instructions, searching existing data sources, gathering and maintaining the data needed, and completing and reviewing the collection of information. Send comments regarding this burden estimate or any other aspect of this collection of information, including suggestions for reducing this burden, to Washington Headquarters Services, Directorate for Information Operations and Reports, 1215 Jefferson Davis Highway, Suite 1204, Arlington, VA 22202-4302, and to the Office of Management and Budget, Paperwork Reduction Project (0704-0188), Washington, DC 20503.				
1. AGENCY USE ONLY (Leave blank)		2. REPORT DATE April 1999	3. REPORT TYPE AND DATES COVERED Contractor Report	
4. TITLE AND SUBTITLE Acoustic Treatment Design Scaling Methods Volume 3: Test Plans, Hardware, Results, and Evaluation			5. FUNDING NUMBERS C-NAS3-26617 TA 25 WU 538-03-12-02	
6. AUTHOR(S) J. Yu, H. W. Kwan, D. K. Echternach, R. E. Kraft, and A. A. Syed				
7. PERFORMING ORGANIZATION NAME(S) AND ADDRESS(ES) General Electric Aircraft Engines (GEAE) P. O. Box 156301 Cincinnati, OH 45215-6301			8. PERFORMING ORGANIZATION REPORT NUMBER Rohr, Inc. Chula Vista, CA	
9. SPONSORING/MONITORING AGENCY NAME(S) AND ADDRESS(ES) National Aeronautics and Space Administration Langley Research Center Hampton, VA 23681-2199			10. SPONSORING/MONITORING AGENCY REPORT NUMBER NASA/CR-1999-209120/VOL3	
11. SUPPLEMENTARY NOTES Lewis Project Manager: Christopher E. Hughes Langley Tech. Monitors: Tony Parrott & Lorenzo Clark Prepared for Langley Research Center under Contract NAS3-26617, Task 25. J. Yu, H. W. Kwan, D. K. Echternach: Rohr, Inc. R. E. Kraft, A. A. Syed: GEAE				
12a. DISTRIBUTION/AVAILABILITY STATEMENT Unclassified-Unlimited Subject Category 71 Availability: NASA CASI (301) 621-0390			12b. DISTRIBUTION CODE	
13. ABSTRACT (Maximum 200 words) The ability to design, build, and test miniaturized acoustic treatment panels on scale-model fan rigs representative of the full-scale engine provides not only a cost-savings, but an opportunity to optimize the treatment by allowing tests of different designs. To be able to use scale model treatment as a full-scale design tool, it is necessary that the designer be able to reliably translate the scale model design and performance to an equivalent full-scale design. The primary objective of the study presented in this volume of the final report was to conduct laboratory tests to evaluate liner acoustic properties and validate advanced treatment impedance models. These laboratory tests include DC flow resistance measurements, normal incidence impedance measurements, DC flow and impedance measurements in the presence of grazing flow, and in-duct liner attenuation as well as modal measurements. Test panels were fabricated at three different scale factors (i.e., full-scale, half-scale, and one-fifth scale) to support laboratory acoustic testing. The panel configurations include single-degree-of-freedom (SDOF) perforated sandwich panels, SDOF linear (wire mesh) liners, and double-degree-of-freedom (DDOF) linear acoustic panels.				
14. SUBJECT TERMS Aircraft noise; acoustic treatment; fan noise suppression; scale models; acoustic impedance			15. NUMBER OF PAGES 81	
			16. PRICE CODE A05	
17. SECURITY CLASSIFICATION OF REPORT Unclassified	18. SECURITY CLASSIFICATION OF THIS PAGE Unclassified	19. SECURITY CLASSIFICATION OF ABSTRACT Unclassified	20. LIMITATION OF ABSTRACT UL	